EUROPEAN JOURNAL OF PURE AND APPLIED MATHEMATICS
2025, Vol. 18, Issue 3, Article Number 6281
ISSN 1307-5543 – ejpam.com
Published by New York Business Global

Applying LPA to Analyze the 3D Motion of a Symmetric Rigid Body with a Large Displacement of a Center of Mass

T. S. Amer[1,*], A. I. Ismail[2], W. S. Amer[3], H. F. El-Kafly[4]

[1] *Mathematics Department, Faculty of Science, Tanta University, Tanta 31527, Egypt*
[2] *Mechanical engineering Department, College of engineering and architecture, Umm Alqura University, Saudi Arabia*
[3] *Mathematics and Computer Science Department, Faculty of Science, Menoufia University, 32511, Egypt*
[4] *Higher Institute of Engineering and Technology, Tanta, Egypt*

Abstract. This study investigates the 3D motion of a rigid body (RB) rotating around a fixed point, focusing on Lagrange's case while considering the effects of a gyrostatic moment (GM) and a Newtonian force field (NFF). It is notably that the center of mass is displaced very much from the principal dynamic symmetry axis. Utilizing the fundamental principle of angular momentum, the equations of motion (EOM) are formulated and solved applying the large parameter approach (LPA) to determine approximate solutions (AS) for the irrational frequencies' case. Euler's angles, which define the body's orientation at any moment, are explicitly calculated. Additionally, to assess the impact of applied moments on motion stability, we utilize advanced computational tools to generate graphical representations of the achieved solutions and the related Euler's angles. This work enhances the understanding of RB dynamics in complex motion scenarios, emphasizing the interaction between external forces and GMs in shaping stability and behavior. The study is poised to greatly influence the aerospace industry by advancing our understanding of rotational motion and the dynamics of celestial bodies, with direct applications in the design and operation of spaceships, spacecraft, and satellites.

2020 Mathematics Subject Classifications: 70E17, 70K45, 34E10, 70F99

Key Words and Phrases: Nonlinear dynamics, Euler's equations, Gyrostatic moment, Perturbation methods, Numerical analysis

*Corresponding author.
DOI: https://doi.org/10.29020/nybg.ejpam.v18i3.6281

Email addresses: tarek.saleh@science.tanta.edu.eg (T. S. Amer), aiismail@uqu.edu.sa (A. I. Ismail), drwaelamer@science.menofia.edu.eg (W. S. Amer), heba_elkafly@yahoo.com (H. F. El-Kafly)

Table 1: List of abbreviations and famous symbols.

RB	*Rigid* body
GM	*Gyrostatic* moment
NFF	*Newtonian* force field
EOM	*Equations* of motion
LPA	*Large* parameter approach
AS	*Approximate* solutions
DEs	$Differential$ equations
$OXYZ$	*Fixed* frame
$Oxyz$	*Rotating* frame
M	$Mass$ of the body
$\underline{\lambda_i}$	*Gyrostatic* moment vector
$\underline{\omega} = (p, q, r)$	*The body's* angular velocity vector
I_1, I_2, I_3	*Principal* moments of inertia
ϵ	*Large* param

1. Introduction

For over two centuries, the study of a RB dynamics has been a focal point of research due to its diverse real-world applications. Gyroscopes, for example, play a critical role in stabilizing and guiding the motion of aircraft, submarines, and spacecraft by maintaining balance and determining orientation. The difficulty of the problem is influenced by the initial conditions, particularly the initial angular velocity, center of mass position, and principal moments of inertia. Moreover, external factors-such as gravitational influences from various centers, whether symmetric or asymmetric, and applied external moments-further complicate the analysis, requiring different mathematical and computational approaches tailored to specific scenarios.

These issues are described by the Euler-Poisson's equations [1], which define the body's angular velocity and orientation at any given time. Extensive research has explored this topic from various perspectives [2–17]. In [2], the motion of the RB subjected to a combination of gyroscopic and axisymmetric potential forces is analyzed, with two integrals of the system provided. In [3], the authors presented a fourth integral associated with the RB motion around a fixed point under the influence of a gravitational moment. Exact solutions to similar problems necessitate a fundamental fourth first integral, which is only derived in specific well-known cases, such as [2–7]. These cases depend on the location of the body's center of mass and the values of its main moments of inertia. In [8] and [9], the authors propose specific conditions for solving the equations of Euler-Poisson and simplify them by transforming the system into three nonlinear differential equations (DEs) involving angular velocity components.

In [10], an innovative method is introduced for solving the Euler-Poisson system, which is well known for its analytical solution challenges. This new method effectively overcomes these difficulties. In [11], the dynamics of a charged the RB rotating about a fixed point

with a rotor attached along a principal axis are examined. The study evaluates sufficient conditions for equilibrium instability using the method of linear approximation. In [12], the spatial rotational motion of a charged symmetric the RB about a stationary point is analyzed, resembling Lagrange's formulation, where the center of mass is displaced slightly from the body's dynamic symmetry axis. In [13], the rotational motion of asymmetric the RB influenced by stationary torques in its body-fixed frame, directed on the first component of the gravitational moment, is analyzed. The study presents analytical results and simulations for two scenarios, where a constant torque is applied along the middle and minor axes. The results are interpreted through separatrix surfaces, periodic and non-periodic solutions, equilibrium manifolds, and the extreme values of periodic solutions. The studies in [14] and [15] focus on the motion of a rotating gyro about a fixed point, analyzed using Lagrange-like criteria. By applying the averaging method, a simplified averaged system for the EOM is derived, taking into account a small parameter. This approach yields AS for two scenarios involving different perturbing moments. The author in [16] further explored the rotational behavior of a symmetric gravitational moment near Lagrange's case, considering the effects of a perturbed torque vector, the third projection of a gravitational moment, and a restoring torque vector. In [17], the PSPM is employed to obtain AS for the motion of the RB in a NFF.

Perturbation methods are highly effective in obtaining AS for similar problems; refer to monographs [18–33]For more details, the Krylov-Bogoliubov-Mitropolski technique is extensively utilized in [18] to derive AS for the EOM of a RB's motion in a gravitational field. However, these solutions include singular points, which are addressed in [19]. In [20–25], the averaging approach is utilized to derive an averaged system for the motion of a symmetric RB from different perspectives. This method is particularly effective in solving the system when the body rotates in a uniform field [20, 21], experiences the GM [22, 23], or involves a charged body [24, 25]. Additionally, in [26], this approach is applied when the center of mass is offset slightly from the axis of dynamic symmetry.

The LPA plays a crucial role in studying symmetric rigid bodies experiencing significant rotational or translational displacements. By defining a dominant parameter that characterizes the motion's scale, AS can be developed to describe the system's core dynamics. This method has been widely applied in fields such as celestial mechanics, robotics, and structural mechanics, where large displacements significantly impact system behavior. In [27, 28], the problem of large RB displacements is examined as a fundamental challenge in classical mechanics and engineering, particularly in relation to nonlinear dynamics and stability. The asymptotic approach based on LPA serves as an effective analytical tool when traditional perturbation methods are insufficient due to strong nonlinearities.

The presented works in [29–31] center broadly on the field of dynamics, with a particular emphasis on the motion of rigid bodies. It covers the core principles of analytical dynamics, spacecraft attitude dynamics, robotics mechanics, perturbation techniques for finding AS, and numerical methods for solving the governing DEs. In [32, 33], the authors solved Euler's equations using three novel approaches to analyze the rotational motion of a charged RB about a fixed point under the influence of GM. Whereas in [34], the authors derived the angular velocity solutions for a RB model, similar to the Lagrange's scenario

with constant torque and GM, by decoupling the EOM and expressing them in complex form. In [35], the authors demonstrate the influence of GMs and the electromagnetic field on the body's motion. In [36], the averaging technique is used to obtain the averaging system of the EOM for a symmetric RB. Notably, this system has been successfully solved for various scenarios, especially when the body moves in a uniform field. The vibrational motions of RBs are studied in several works, e.g. [37–40]. The planar dynamics of an elastic spring connected to a RB are analyzed in [37], leading to a dynamical model with three-degree-of-freedom that follows the same path as its point of suspension. In [38], a particular case is explored where the suspension point remains fixed. The study in [39] examines linear damped spring that carry a RB, with the pivot point tracing an elliptical path. These works employ the method of multiple-scales to obtain the AS of the EOM. Consequently, solvability requirements are derived by eliminating secular terms, and potential resonance cases are defined. In [40], the vibrational behavior of a rigid body around its equilibrium position is investigated numerically using the ode45 solver, based on the fourth-order Runge-Kutta method [41]. The comparison between numerical solutions and asymptotic solutions for the pendulum motions of RBs is presented in [42], demonstrating their reliability and the high accuracy of the perturbation approach utilized. A generalization of this problem is discussed in [43]. Additionally, the Routh-Hurwitz criteria [44] are applied to confirm the stability of steady-state solutions and to assess their various stability regions.

The presented works in [45–48] demonstrate innovative approaches to solving intricate mechanical systems, enhancing the precision and applicability of mathematical models in physics and engineering. In [45], a comparative study of analytical and numerical solutions for a mass-spring system on a massless cart, revealing dynamic interactions that enhance understanding in mechanical engineering contexts is presented. In [46], the authors explored a pendulum situated between two springs using the Ms-DTM method, shedding light on complex dynamic behaviors and the efficacy of this analytical technique. A theoretical study of harmonic oscillators applying the optimal and modified homotopy method is examined in [47] to address time dependence, contributing valuable insights into dynamic system analysis. Moreover, examine a pendulum's response to vibratory influences using semi-analytical solutions formed through the aforementioned method is examined in [48]. A comprehension of pendulum dynamics and validating sophisticated perturbation techniques within mechanical problems is presented.

The work explores the 3D motion of a symmetric the RB with a very much displacement of its center of mass from the axis of dynamic symmetry. The system is subjected to the GM and a NFF. The LPA is employed to obtain AS for the EOM in cases of irrational frequencies. Such solutions are then visualized to highlight the influence of various body parameters on the motion over time, serving as a generalization of earlier work [16]. The use of the LPA enables the derivation of AS remain valid even for significant deviations from equilibrium. Recent advancements in asymptotic methods have proven effective in addressing highly nonlinear the RB problems. Euler's angles for the motion are determined, and graphical representations provide insight into the motion at any given instant. The significance of this work explores the mathematical formulation, derivation, and ap-

plications of the LPA in solving large displacement problems for symmetric the RBs. By leveraging asymptotic approximations, we aim to provide practical and computationally efficient solutions to highly nonlinear the RB problems, contributing to both theoretical and applied mechanics.

The RB dynamics play a significant role in the theory of gyroscopes, particularly for symmetric RBs that rotate rapidly around their axis of symmetry. Gyroscopes are crucial in numerous engineering applications. For instance, in racing vehicles, the engine itself acts like a large gyroscope, influencing performance and stability. In aviation, gyroscopes help maintain stability and control orientation; when an aircraft turns right or left, the gyroscopic effect can cause the nose or tail to rise or dip accordingly. Similarly, gyroscopes are essential for steering and pitching in ships. There are various types of gyroscopes used to measure angular velocity, including optical, vibrating, and mechanical gyroscopes. Micromechanical gyroscopes are widely used in consumer electronics, as well as in compasses, computer pointing devices, and other systems requiring orientation detection.

2. Overview of the problem

This section aims to offer a deeper insight into the dynamic behavior of a heavy symmetric RB with mass M , such as the conditions of Lagrange's gyroscope are satisfied. The body is anchored at a point O, which serves as the origin for two coordinate systems: a stationary one $OXYZ$ and a rotating one $Oxyz$ that is rigidly attached to the body, with its axes aligned along the inertia's main axes at O. We will suppose that the body is influenced by a GM $\underline{\lambda}$, whose components $(\lambda_j; j = 1, 2, 3)$ are directed on the principal axes Ox, Oy and OZ. Additionally,in which $\lambda_1 = 0$ and a NFF originating from an attracting center O_1, located along the downward fixed axis OZ and far away the origin O, at a significant distance R (see Fig. (1)).

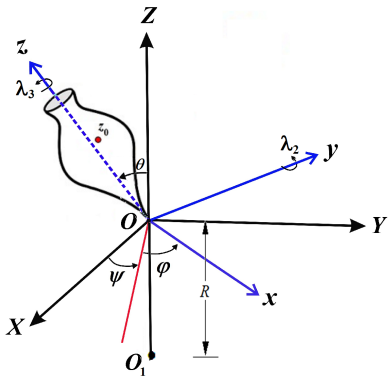

Figure 1: The RB's problem.

The EOM are formulated according to the equations Euler-Poisson's [1], as follows

$$\begin{gathered} I_1\dot{p}-(I_2-I_3)qr+q\lambda_3-r\lambda_2=Mg(\gamma y_G-\beta z_G)-N(I_2-I_3)\beta\gamma,\\ I_2\dot{q}-(I_3-I_1)rp-p\lambda_3=Mg(\alpha z_G-\gamma x_G)-N(I_3-I_1)\gamma\alpha,\\ I_3\dot{r}-(I_1-I_2)pq+p\lambda_2=Mg(\beta x_G-\alpha y_G)-N(I_1-I_2)\alpha\beta,\\ \dot{\alpha}=r\beta-q\gamma,\quad \dot{\beta}=p\gamma-r\alpha,\quad \dot{\gamma}=q\alpha-p\beta. \end{gathered} \tag{1}$$

It is important to note that the inertia principal moments are denoted by I_j along the principal axes. The over dots indicate derivatives regarding time t, g denotes gravitational acceleration, $N=3g/R$ and ϵ represent a large parameter. In this context, (p,q,r) , (α,β,γ), and $x_G,y_G,z_G)$ refer to the angular velocity's components, the unit vector along the vertical Z-axis, and the center of mass coordinates in the principal axis frame, respectively. The given EOM have three first integrals associated with energy, area, and geometric one [1]

$$\begin{gathered} I_1p^2+I_2q^2+I_3r^2-2Mg(\alpha x_G+\beta y_G+\gamma z_G)+N(I_1\alpha^2+I_2\beta^2+I_3\gamma^2)\\ =I_1p_0^2+I_2q_0^2+I_3r_0^2-2Mg(\alpha_0x_G+\beta_0y_G+\gamma_0z_G)+N(I_1\alpha_0^2+I_2\beta_0^2+I_3\gamma_0^2),\\ I_1p\alpha+(I_2q+\lambda_2)\beta+(I_3r+\lambda_3)\gamma=I_1p_0\alpha_0+(I_2q_0+\lambda_2)\beta_0+(I_3r_0+\lambda_3)\gamma_0,\\ \alpha^2+\beta^2+\gamma^2=1, \end{gathered} \tag{2}$$

where $p_0,q_0,r_0,\alpha_0,\beta_0$ and γ_0 represent the values of p,q,r,α,β and γ and $t=0$, respectively.

Taking the following parameters and variables into consideration:

$$\begin{gathered} \sqrt{\varepsilon}p=\tfrac{p_1}{n},\quad \sqrt{\varepsilon}q=\tfrac{q_1}{n},\quad r=\tfrac{r_1}{n},\quad \sqrt{\varepsilon}\alpha=\alpha_1,\quad \sqrt{\varepsilon}\ \beta=\beta_1,\\ \gamma=\gamma_1,\quad \sqrt{\varepsilon}\ \lambda_2=\tfrac{I_2}{n}\acute{\lambda_2},\quad \lambda_3=\tfrac{I_3}{n}\acute{\lambda_3},\quad t=n\tau,\\ n=\sqrt{I_1/Mgz_G},\quad a=(I_1-I_3)/I_1,\quad b=I_3/I_1,\\ I_1=I_2\neq I_3,\quad \sqrt{\varepsilon}x_G=z_G,\quad y_G=0,\quad k=Nan^2. \end{gathered} \tag{3}$$

Upon substituting (3) into (1) and (2), the following equivalent system is obtained

$$\begin{gathered} \tfrac{dp_1}{d\tau}=aq_1r_1+r_1\acute{\lambda_2}-q_1\acute{\lambda_3}-\beta_1-k\beta_1\gamma_1,\\ \tfrac{dq_1}{d\tau}=-ap_1r_1+p_1\acute{\lambda_3}+\alpha_1-\gamma_1+k\alpha_1\gamma_1,\\ \varepsilon\tfrac{dr_1}{d\tau}=-(p_1\acute{\lambda_2}-\tfrac{1}{b}\beta_1),\\ \tfrac{d\alpha_1}{d\tau}=r_1\beta_1-q_1\gamma_1,\quad \tfrac{d\beta_1}{d\tau}=p_1\gamma_1-r_1\alpha_1,\quad \varepsilon\ \tfrac{d\gamma_1}{d\tau}=(q_1\alpha_1-p_1\beta_1), \end{gathered} \tag{4}$$

$$\begin{gathered} p_1^2+q_1^2-2\alpha_1+\varepsilon(br_1^2-2\gamma_1-k\gamma_1^2)=p_{10}^2+q_{10}^2-2\alpha_{10}+\varepsilon(br_{10}^2-2\gamma_{10}-k\gamma_{10}^2),\\ p_1\alpha_1+(q_1+\acute{\lambda_2})\beta_1+\varepsilon(br_1+\acute{\lambda_3})\gamma_1=p_{10}\alpha_{10}+(q_{10}+\acute{\lambda_2})\beta_{10}+\varepsilon(br_{10}+\acute{\lambda_3})\gamma_{10},\\ \alpha_1^2+\beta_1^2+\varepsilon\gamma_1^2=\varepsilon. \end{gathered} \tag{5}$$

3. The used approach

This section aims to apply the LPA [27, 28] to achieve the solutions for the RB under investigation. To achieve this aim, we can use the above first integrals to represent $r_1$andγ_1, as follows

$$\varepsilon r_1=\varepsilon r_{10}-u_2,\quad \varepsilon\gamma_1=\varepsilon-u_1, \tag{6}$$

where

$$\begin{gathered} u_1 = \tfrac{1}{8}(4U_1 + \varepsilon^{-1}U_1^2) + ..., \\ u_2 = \tfrac{1}{8br_{10}}\{r_{10}^2[4(U_2 - U_{20}) + \varepsilon^{-1}(U_1^2 - U_{10}^2)] + \tfrac{\varepsilon^{-2}}{br_{10}^2}(U_2 - U_{20})^2 + ...\}, \\ U_1 = \alpha_1^2 + \beta_1^2, \qquad U_2 = p_1^2 + q_1^2 - 2\alpha_1 + U_1(k+1). \end{gathered} \tag{7}$$

Here, $U_{s0}; (s = 1, 2)$ stands for the values of U_s at $t = 0$, whereas the dots represent small terms of higher-order powers of ε^{-1} .

To refine system (4) into a more practical form, we remove r_1 and γ_1 from (4). By incorporating (6) into (4), yields the following nonlinear system of first-order differential equations

$$\begin{gathered} \varepsilon\tfrac{dp_2}{d\tau} = \varepsilon\acute{\lambda_2}r_{10}(1 + \chi\delta) + \varepsilon\rho_1 q_2 + N_1, \qquad \varepsilon\tfrac{dq_2}{d\tau} = -\varepsilon\rho_1 p_2 + N_2, \\ \varepsilon\tfrac{d\alpha_2}{d\tau} = \varepsilon\delta\acute{\lambda_2}r_{10} + \varepsilon\rho_2\beta_2 + N_3, \qquad \varepsilon\tfrac{d\beta_2}{d\tau} = -\varepsilon\rho_2\alpha_2 + N_4, \end{gathered} \tag{8}$$

where

$$\begin{gathered} p_1 = p_2 + \chi\alpha_2 + d_1, \\ q_1 = q_2 + \chi\beta_2, \\ \alpha_1 = (1 + \chi\delta)\alpha_2 + \delta p_2 + d_2, \\ \beta_1 = (1 + \chi\delta)\beta_2 + \delta q_2, \\ \chi = -(1 + k)/ \pm \sqrt{(br_{10} + \acute{\lambda_3})^2 + 4(1 + k)}, \\ \delta = [-(br_{10} + \acute{\lambda_3}) \pm \sqrt{(br_{10} + \acute{\lambda_3})^2 + 4(1 + k)}]/2(1 + k), \\ d_1 = r_{10}/(1 + k + r_{10}\acute{\lambda_3} - ar_{10}^2), \qquad d_2 = d_1/r_{10}, \\ \rho_1 = \chi(1 - r_{10}\delta) + (ar_{10} - \delta(1 + k) - \acute{\lambda_3})(1 + \chi\delta), \\ \rho_2 = \chi[\delta(\acute{\lambda_3} - ar_{10}) - 1] + (r_{10} + \delta(1 + k))(1 + \chi\delta), \\ N_1 = \chi(u_2\beta_1 - q_1u_1) - (1 + \chi\delta)[(aq_1 + \acute{\lambda_2})u_2 - ku_1\beta_1], \\ N_2 = \chi(u_1p_1 - u_2\alpha_1) + (1 + \chi\delta)[ap_1u_2 + u_1 - k\alpha_1u_1], \\ N_3 = \delta[(aq_1 + \acute{\lambda_2})u_2 - ku_1\beta_1] - (u_2\beta_1 - u_1q_1), \\ N_4 = -\delta[ap_1u_2 + u_1 - ku_1\beta_1] - (u_1p_1 - u_2\alpha_1). \end{gathered} \tag{9}$$

To better understand the distribution of frequencies $\rho_s; (s = 1, 2)$,we choose a suitable value for r_0. Consequently, ρ_1/ρ_2 may be treated as a rational number, leading to a solution of system (8) that is periodic with a period $(T_0 = 2\pi n_s/\rho_s; \quad s = 1, 2)$.

Next, we reformulate the problem to identify the $\tau_0(\varepsilon)$ solutions of system (8) with a significantly large value of ε. In this context, $\varepsilon \to \infty$ should approach a solution of period T_0 of the generating system (8). Therefore, we introduce the following substitution:

$$\varepsilon\tau = (\varepsilon + \mu)T, \tag{10}$$

in which $\mu = \mu(\varepsilon)$ that will be estimated latter.

Consequently, the problem under investigation is simplified to finding the solutions for the period T_0 of the following system

$$\begin{gathered} \varepsilon\tfrac{dp_2}{dT} = \varepsilon(1 + \chi\delta)\acute{\lambda_2}r_{10} + \varepsilon\rho_1 q_2 + V_1, \quad \varepsilon\tfrac{dq_2}{dT} = -\varepsilon\rho_1 p_2 + V_2, \\ \varepsilon\tfrac{d\alpha_2}{dT} = \varepsilon\delta\acute{\lambda_2}r_{10} + \varepsilon\rho_2\beta_2 + V_3, \qquad \varepsilon\tfrac{d\beta_2}{d\tau} = -\varepsilon\rho_2\alpha_2 + V_4, \end{gathered} \tag{11}$$

where

$$\begin{gathered}\varepsilon V_1 = \varepsilon[(1+\chi\delta)\acute{\lambda_2} r_{10} + \rho_1 q_2]\mu + (\varepsilon+\mu)N_1, \\ \varepsilon V_2 = -\varepsilon\rho_1\mu p_2 + (\varepsilon+\mu)N_2, \\ \varepsilon V_3 = \varepsilon(\delta\acute{\lambda_2} r_{10} + \rho_2\beta_2)\mu + (\varepsilon+\mu)N_3, \\ \varepsilon V_4 = -\varepsilon\rho_2\alpha_2\mu + (\varepsilon+\mu)N_4, \\ V_i = V_i^{(1)} + \varepsilon^{(-1)}V_i^{(2)} + \varepsilon^{-2}V_i^3 + ...\end{gathered} \tag{12}$$

We will now proceed to derive the solutions for system (11). Upon closer examination, we observe that this system constitutes a dynamical system comprised of first-order nonlinear DEs involving the variables p_2, q_2, γ_2 and β_2. By differentiating these equations once more, we can generate a new system of second-order DEs, which can be expressed as follows

$$\begin{gathered}\varepsilon(\tfrac{d^2p_2}{dT^2} + \rho_1^2 p_2) = \rho_1 V_2 + \dot{V_1}, \\ \varepsilon(\tfrac{d^2q_2}{dT^2} + \rho_1^2 q_2) = (-\rho_1 V_1 + \dot{V_2}) - \varepsilon(1+\chi\delta)\rho_1\acute{\lambda_2} r_{10}, \\ \varepsilon(\tfrac{d^2\alpha_2}{dT^2} + \rho_2^2\alpha_2) = (\rho_2 V_4 + \dot{V_3}), \\ \varepsilon(\tfrac{d^2\beta_2}{dT^2} + \rho_2^2\beta_2) = (-\rho_2 V_3 + \dot{V_4}) - \varepsilon\rho_2\delta\acute{\lambda_2} r_{10}.\end{gathered} \tag{13}$$

The aforementioned system comprises four distinct nonlinear DEs, each containing a single variable. With this analysis in mind, we can pursue the solutions of this system as follows

$$\begin{gathered}p_2(T,\varepsilon) = A_1\cos\rho_1 T + A_2\sin\rho_1 T + \textstyle\sum_1, \\ q_2(T,\varepsilon) = -A_1\sin\rho_1 T + A_2\cos\rho_1 T - [(1+\chi\delta)\acute{\lambda_2} r_{10}]/\rho_1 + \textstyle\sum_2, \\ \alpha_2(T,\varepsilon) = A_3\cos\rho_2 T + \textstyle\sum_3, \\ \beta_2(T,\varepsilon) = -A_3\sin\rho_2 T - \delta\acute{\lambda_2} r_{10}/\rho_2 + \textstyle\sum_4, \\ (\textstyle\sum_d = \sum_{n=1}^{\infty}\varepsilon^{-n}D_d^{(n)}(T); d = 1,2,3,4),\end{gathered} \tag{14}$$

with the following initial conditions

$$\begin{gathered}p_2(0,\varepsilon) = A_1 = A_1^{(0)} + a_1, \\ q_2(0,\varepsilon) = A_2 - [(1+\chi\delta)\acute{\lambda_2} r_{10}]/\rho_1 = A_2^{(0)} + a_2 - [(1+\chi\delta)\acute{\lambda_2} r_{10}]/\rho_1, \\ \alpha_2(0,\varepsilon) = A_3 = A_3^{(0)} + a_3, \\ \beta_2(0,\varepsilon) = -\delta\acute{\lambda_2} r_{10}/\rho_2.\end{gathered} \tag{15}$$

In this context,$A_j^{(0)}$ and $a_j; (j = 1, 2.3)$ represent the unperturbed and perturbed components A_j , respectively.

It is notably that the solutions of system (8), which have T_0-periodic solutions in system (13), exhibit a period of $\varepsilon T_1 = (\varepsilon+\mu)T_0$. We will assume that $\mu = \mu_0 + a_4$ has solutions of the form (14) that are periodic, seeking $a_d = a_d(\varepsilon); d = 1,2,3,4$ as a function of the large parameter ε that approaches zero as $\varepsilon \to \infty$. In accordance with the LPA procedure, we modify the initial conditions to correspond with the arbitrary constants in the generating system's solutions. Utilizing equations (9) and (7), we obtain the following

results

$$\begin{aligned}
U_1^{(0)} &= d_2^2+\delta^2(A_1^2+A_2^2)+(1+\chi\delta)^2A_3^2+2\delta d_2(A_1\cos\rho_1T+A_2\sin\rho_1T)\\
&+2d_2(1+\chi\delta)A_3\cos\rho_2T+2\delta(1+\chi\delta)A_3[A_1\cos(\rho_1-\rho_2)T+A_2\\
&\times\sin(\rho_1-\rho_2)T]+2\delta^2(1+\chi\delta)\acute{\lambda_2}r_{10}(\tfrac{\rho_1+\rho_2}{\rho_1\rho_2})(A_1\sin\rho_1T-A_2\cos\rho_1T)\\
&+2\delta(1+\chi\delta)^2\acute{\lambda_2}r_{10}(\tfrac{\rho_1+\rho_2}{\rho_1\rho_2})A_3\sin\rho_2T+\delta^2(1+\chi\delta)^2(\acute{\lambda_2}r_{10})^2\\
&\times(\tfrac{\rho_1+\rho_2}{\rho_1\rho_2})^2,\\
U_2^{(0)} &= d_1^2+(A_1^2+A_2^2)+\chi^2A_3^2-2d_2+2(d_1-\delta)(A_1\cos\rho_1T+A_2\sin\rho_1T)\\
&+2(d_1\chi-1-\chi\delta)A_3\cos\rho_2T+U_1^{(0)}(1+k)+2\chi A_3[A_1\cos(\rho_1-\rho_2)T\\
&+A_2\sin(\rho_1-\rho_2)T]+\acute{\lambda_2}r_{10}[\tfrac{\chi\delta(\rho_1+\rho_2)+\rho_2}{\rho_1\rho_2}][2(A_1\sin\rho_1T-A_2\cos\rho_1T)\\
&+2\chi\acute{\lambda_2}r_{10}\tfrac{\rho_1\chi\delta+\rho_2(1-\chi\delta)}{\rho_1\rho_2}A_3\sin\rho_2T+(\acute{\lambda_2}r_{10})^2(\tfrac{\chi\delta(\rho_1+\rho_2)+\rho_2}{\rho_1\rho_2})^2].
\end{aligned}\tag{16}$$

The expressions for $N_d;(d=1,2,3,4)$ in (9) can be reformulated in the form

$$\begin{aligned}
N_1&=\Lambda_1q_2+\Lambda_2\beta_2+\Lambda_3, \quad & N_2&=-(\Lambda_1p_2+\Lambda_2\alpha_2)+\Lambda_4,\\
N_3&=\Lambda_5q_2+\Lambda_6\beta_2+\Lambda_7, \quad & N_4&=-(\Lambda_5p_2+\Lambda_6\alpha_2)+\Lambda_8,
\end{aligned}\tag{17}$$

where

$$\begin{aligned}
\Lambda_1&=-a(1+\chi\delta)u_2+\chi(\delta u_2-u_1)+k\beta(1+\chi\delta)u_1,\\
\Lambda_2&=-\chi a(1+\chi\delta)u_2-\chi[\chi u_1-(1+\chi\delta)u_2]+k\beta(1+\chi\delta)^2u_1,\\
\Lambda_3&=-(1+\chi\delta)\acute{\lambda_2}u_2,\\
\Lambda_4&=(1+\chi\delta)[ad_1u_2+u_1(1-kd_2)]+\chi(d_1u_1-d_2u_2),\\
\Lambda_5&=\delta u_2(a-1)+u_1(1-k\delta^2),\\
\Lambda_6&=\chi(\delta au_2+u_1)-(1+\chi\delta)(u_2-ku_1),\\
\Lambda_7&=\delta\acute{\lambda_2}u_2,\\
\Lambda_8&=-\delta[au_2d_1+u_1(1-kd_2)]-(d_1u_1-d_2u_2).
\end{aligned}\tag{18}$$

Using the aforementioned equations, the unperturbed notations of $\Lambda_l;(l=1,2,...,8)$are written as:

$$\begin{aligned}
\Lambda_l^{(0)}&=\left[\Gamma_{l1}+\Gamma_{l2}\left(A_1^2+A_2^2\right)+\Gamma_{l3}A_3^2\right]+\Gamma_{l4}\left(A_1\cos\rho_1T+A_2\sin\rho_1T\right)\\
&+\Gamma_{l5}A_3\cos\rho_2T+\Gamma_{l6}A_3\left[A_1\cos\left(\rho_1-\rho_2\right)T+A_2\sin\left(\rho_1-\rho_2\right)T\right]\\
&+\Gamma_{l7}\left(A_1\sin\rho_1T-A_2\cos\rho_1T\right)+\Gamma_{l8}A_3\sin\rho_1T
\end{aligned}\tag{19}$$

Where Γ_{lr} represents elements of the square matrix$\|\ \Gamma_{lr}\ \|;(l,r=1,2,3,...,8)$. To determine these elements, substitute $U_1^{(0)},U_2^{(0)}$ into equation (7) to obtain $u_1^{(0)}$ and $u_2^{(0)}$. Consequently, $\Gamma_{1r},\Gamma_{2r},...,\Gamma_{8r}$ can be obtained smoothly (see Appendix I).

By examining the solutions in equation (14), it becomes clear that these solutions can be achieved if $D_d^{(n)}(T)$ are calculated. By inserting the solutions (14) into system (11) and equaling the coefficients of corresponding powers of ε^{-1} on both sides, we derive a system

that defines the coefficients $D_d^{(n)}(T)$ in (14) as follows

$$\begin{array}{l} \frac{dD_1^{(n)}}{dT} = \rho_1 D_2^{(n)}(T) + V_1^{(n)}(T), \\ \frac{dD_2^{(n)}}{dT} = -\rho_1 D_1^{(n)}(T) + V_2^{(n)}(T), \\ \frac{dD_3^{(n)}}{dT} = \rho_2 D_4^{(n)}(T) + V_3^{(n)}(T), \\ \frac{dD_4^{(n)}}{dT} = -\rho_2 D_3^{(n)}(T) + V_4^{(n)}(T), \end{array} \tag{20}$$

where the conditions $D_d^{(n)}(0) = 0$, are considered and $V_d^{(n)}(T)$ represent known functions, if $D_d^{(e)}$ is estimated for $e < n$.

At $n = 1$: Introducing V_d from (12) into (20), matching the coefficients of similar powers of ε^{-1} on both sides, and differentiating the resulting equations regarding T , we obtain the following equations that determine $D_d^{(1)}(T)$

$$\begin{array}{l} \frac{d^2D_1^{(1)}}{dT^2} + \rho_1^2 D_1^{(1)}(T) = \Theta_{11}(T), \\ \frac{d^2D_2^{(1)}}{dT^2} + \rho_1^2 D_2^{(1)}(T) = \Theta_{21}(T), \\ \frac{d^2D_3^{(1)}}{dT^2} + \rho_2^2 D_3^{(1)}(T) = \Theta_{31}(T), \\ \frac{d^2D_4^{(1)}}{dT^2} + \rho_2^2 D_4^{(1)}(T) = \Theta_{41}(T), \end{array} \tag{21}$$

where,

$$\begin{aligned} \Theta_{11}(T) &= -2\rho_1(\rho_1\mu_0 + \Lambda_1^{(0)})p_2^{(0)} - (\rho_1+\rho_2)\Lambda_2^{(0)}\alpha_2^{(0)} + \tfrac{d\Lambda_1^{(0)}}{dT}q_2^{(0)} \\ &\quad + \tfrac{d\Lambda_2^{(0)}}{dT}\beta_2^{(0)} + \rho_1\Lambda_4^{(0)} + \tfrac{d\Lambda_3^{(0)}}{dT}, \\ \Theta_{21}(T) &= -2\rho_1(\rho_1\mu_0 + \Lambda_1^{(0)})q_2^{(0)} - (\rho_1+\rho_2)\Lambda_2^{(0)}\beta_2^{(0)} - \tfrac{d\Lambda_1^{(0)}}{dT}p_2^{(0)} \\ &\quad - \tfrac{d\Lambda_2^{(0)}}{dT}\alpha_2^{(0)} + \tfrac{d\Lambda_4^{(0)}}{dT} - 2\rho_1\acute{\lambda_2}r_{10}(1+\chi\delta)\mu_0 - \acute{\lambda_2}r_{10}(1+\chi\delta)\Lambda_1^{(0)} \\ &\quad - \delta\acute{\lambda_2}r_{10}\Lambda_2^{(0)} - \rho_1\Lambda_3^{(0)}, \\ \Theta_{31}(T) &= -2\rho_2(\rho_2\mu_0 + \Lambda_6^{(0)})\alpha_2^{(0)} - (\rho_1+\rho_2)\Lambda_5^{(0)}p_2^{(0)} + \tfrac{d\Lambda_5^{(0)}}{dT}q_2^{(0)} \\ &\quad + \tfrac{d\Lambda_6^{(0)}}{dT}\beta_2^{(0)} + \rho_2\Lambda_8^{(0)} + \tfrac{d\Lambda_7^{(0)}}{dT}, \\ \Theta_{41}(T) &= -2\rho_2(\rho_2\mu_0 + \Lambda_6^{(0)})\beta_2^{(0)} - (\rho_1+\rho_2)q_2^{(0)} - 2\rho_2\delta\acute{\lambda_2}r_{10}\mu_0 - \delta\acute{\lambda_2}r_{10}\Lambda_6^{(0)} \\ &\quad - \acute{\lambda_2}r_{10}(1+\chi\delta)\Lambda_5^{(0)} - \rho_2\Lambda_7^{(0)} - \tfrac{d\Lambda_5^{(0)}}{dT}p_2^{(0)} - \tfrac{d\Lambda_6^{(0)}}{dT}\alpha_2^{(0)} + \tfrac{d\Lambda_8^{(0)}}{dT}. \end{aligned}$$

Knowing that $\Theta_{d1}(u)$, the solutions of the previous system(21) take the form

$$\begin{array}{l} D_1^{(1)}(T) = \rho_1^{-1}\int_0^T \Theta_{11}(v)\sin\rho_1(T-v)dv, \\ D_2^{(1)}(T) = \rho_1^{-1}\int_0^T \Theta_{21}(v)\sin\rho_1(T-v)dv, \\ D_3^{(1)}(T) = \rho_2^{-1}\int_0^T \Theta_{31}(v)\sin\rho_2(T-v)dv, \\ D_4^{(1)}(T) = \rho_2^{-1}\int_0^T \Theta_{41}(v)\sin\rho_2(T-v)dv, \end{array} \tag{22}$$

where,

$$\begin{aligned}
\rho_1^{-1}\Theta_{11}(T) &= G_{10} + G_{11}\left(A_1\cos\rho_1 T + A_2\sin\rho_1 T\right) + G_{12}\left(A_1\cos\rho_1 T - A_2\sin\rho_1 T\right)\\
&+ G_{13}\cos 2\rho_1 T + G_{14}\sin 2\rho_1 T + G_{15}A_3\cos\rho_2 T\\
&+ G_{16}A_3\left[A_1\cos(\rho_1-\rho_2)T + A_2\sin(\rho_1-\rho_2)T\right]\\
&+ G_{17}A_3\left[A_1\cos(\rho_1-\rho_2)T - A_2\sin(\rho_1-\rho_2)T\right]\\
&+ G_{18}A_3\left[A_1\cos(\rho_1+\rho_2)T + A_2\sin(\rho_1+\rho_2)T\right]\\
&- G_{19}A_3\left[A_1\cos(\rho_1+\rho_2)T - A_2\sin(\rho_1+\rho_2)T\right]\\
&+ G_{110}\cos(2\rho_1-\rho_2)T + G_{111}\sin(2\rho_1-\rho_2)T\\
&+ G_{112}A_3^2\left[A_1\cos(\rho_1-2\rho_2)T + A_2\sin(\rho_1-2\rho_2)T\right]\\
&+ G_{113}A_3^2\left[A_1\cos(\rho_1-2\rho_2)T - A_2\sin(\rho_1-2\rho_2)T\right]\\
&+ G_{114}\cos 2\rho_2 T + G_{115}\sin 2\rho_2 T + G_{116}A_3\left[A_1\sin(\rho_1-\rho_2)T - A_2\cos(\rho_1-\rho_2)T\right]\\
&+ G_{117}A_3\left[A_1\sin(\rho_1-\rho_2)T + A_2\cos(\rho_1-\rho_2)T\right]\\
&+ G_{118}A_3\left[A_1\sin(\rho_1+\rho_2)T + A_2\cos(\rho_1+\rho_2)T\right]\\
&+ G_{119}A_3\left[A_1\sin(\rho_1+\rho_2)T - A_2\cos(\rho_1+\rho_2)T\right]\\
&+ G_{120}A_3A_2\left[\cos(\rho_1+\rho_2)T + \cos(\rho_1-\rho_2)T\right]\\
&+ G_{121}\left(A_1\sin\rho_1 T - A_2\cos\rho_1 T\right) + G_{122}A_3\sin 2\rho_2 T\\
&+ G_{123}\sin(\rho_1-\rho_2)T,\\
\rho_1^{-1}\Theta_{21}(T) &= G_{20} - G_{21}\left(A_1\sin\rho_1 T - A_2\cos\rho_1 T\right)\\
&+ G_{22}\left(A_1\sin\rho_1 T + A_2\cos\rho_1 T\right) + G_{23}\left(A_1\cos\rho_1 T + A_2\sin\rho_1 T\right)\\
&- G_{24}A_3\sin\rho_2 T - G_{25}A_3\left[A_1\sin(\rho_1-\rho_2)T - A_2\cos(\rho_1-\rho_2)T\right]\\
&+ G_{26}A_3\left[A_1\cos(\rho_1-\rho_2)T - A_2\sin(\rho_1-\rho_2)T\right]\\
&+ G_{27}A_3\left[A_1\cos(\rho_1-\rho_2)T + A_2\sin(\rho_1-\rho_2)T\right]\\
&+ G_{28}A_3\left[A_1\sin(\rho_1-\rho_2)T + A_2\cos(\rho_1-\rho_2)T\right]\\
&- G_{29}A_3\left[A_1\sin(\rho_1+\rho_2)T - A_2\cos(\rho_1-\rho_2)T\right]\\
&+ G_{210}A_3\left[A_1\sin(\rho_1+\rho_2)T + A_2\cos(\rho_1+\rho_2)T\right]\\
&+ G_{211}A_3\left[A_1\cos(\rho_1+\rho_2)T - A_2\sin(\rho_1+\rho_2)T\right]\\
&+ G_{212}A_3\left[A_1\cos(\rho_1+\rho_2)T + A_2\sin(\rho_1+\rho_2)T\right]\\
&+ G_{213}\sin(2\rho_1-\rho_2)T + G_{214}A_3^2\left[A_1\sin(\rho_1-2\rho_2)T + A_2\cos(\rho_1-2\rho_2)T\right]\\
&+ G_{215}A_3^2\left[A_1\sin(\rho_1-2\rho_2)T - A_2\cos(\rho_1-2\rho_2)T\right]\\
&- G_{216}\sin 2\rho_2 T + G_{217}A_3\cos\rho_2 T\\
&+ G_{218}A_3^2\cos 2\rho_2 T,\\
\rho_2^{-1}\Theta_{31}(T) &= G_{30} + G_{31}A_3\sin\rho_2 T + G_{32}A_3\cos\rho_2 T\\
&+ G_{33}A_3^2\sin 2\rho_2 T + G_{34}A_3^2\cos 2\rho_2 T,
\end{aligned}$$

$$\begin{aligned}\rho_2^{-1}\Theta_{41}(T) = {} & G_{40} - G_{41}\left(A_1 \sin \rho_1 T - A_2 \cos \rho_1 T\right) \\ & + G_{42}\left(A_1 \sin \rho_1 T + A_2 \cos \rho_1 T\right) + G_{43}\left(A_1 \cos \rho_1 T + A_2 \sin \rho_1 T\right) \\ & - G_{44} \sin 2\rho_1 T + G_{45} \cos 2\rho_1 T - G_{46} A_3 \sin \rho_2 T \\ & - G_{47} A_3 \left[A_1 \sin(\rho_1 - \rho_2)T - A_2 \cos(\rho_1 - \rho_2)T\right] \\ & + G_{48} A_3 \left[A_1 \sin(\rho_1 - \rho_2)T + A_2 \cos(\rho_1 - \rho_2)T\right] \\ & + G_{49} A_3 \left[A_1 \cos(\rho_1 - \rho_2)T + A_2 \sin(\rho_1 - \rho_2)T\right] \\ & + G_{410} A_3 \left[A_1 \cos(\rho_1 - \rho_2)T - A_2 \sin(\rho_1 - \rho_2)T\right] \\ & - G_{411} A_3 \left[A_1 \sin(\rho_1 + \rho_2)T - A_2 \cos(\rho_1 + \rho_2)T\right] \\ & + G_{412} A_3 \left[A_1 \sin(\rho_1 + \rho_2)T + A_2 \cos(\rho_1 + \rho_2)T\right] \\ & + G_{413} A_3 \left[A_1 \cos(\rho_1 + \rho_2)T + A_2 \sin(\rho_1 + \rho_2)T\right] \\ & + G_{414} A_3 \left[A_1 \cos(\rho_1 + \rho_2)T - A_2 \sin(\rho_1 + \rho_2)T\right] \\ & + G_{415} \sin(2\rho_1 - \rho_2)T + G_{416} \cos(2\rho_1 - \rho_2)T \\ & - G_{417} A_3^2 \left[A_1 \sin(\rho_1 - 2\rho_2)T - A_2 \cos(\rho_1 - 2\rho_2)T\right] \\ & + G_{418} A_3^2 \left[A_1 \sin(\rho_1 - 2\rho_2)T + A_2 \cos(\rho_1 - 2\rho_2)T\right] \\ & - G_{419} \sin(2\rho_2)T + G_{420} A_3 \cos(\rho_2 T) \\ & + G_{421} \cos(2\rho_2)T.\end{aligned}$$

Here $G_{1h}(h = 0, 1, 2, ..., 23), G_{2z}(z = 0, 1, 2, ..., 18), G_{3k}(k = 0, 1, 2, 3, 4)$ and $(G_{4u}; u = 0, 1, 2, ..., 21)$ are constants can be acquired easily (see Appendix 2).

Substitution of $\Theta_{d1}(u)$ into (22), yields

$$\begin{aligned} D_1^{(1)}(T_0) &= (E_{11} + R_{11})T_0, \\ D_2^{(1)}(T_0) &= (E_{21} + R_{21})T_0, \\ D_4^{(1)}(T_0) &= -(E_{31} + R_{41})T_0, \end{aligned} \tag{23}$$

where

$$\begin{aligned} E_{11} &= -\tfrac{1}{2}[(G_{11} - G_{12})A_2 + G_{121}A_1], \\ E_{21} &= -\tfrac{1}{2}[(G_{23} - G_{21})A_1 + G_{22}A_2], \\ E_{31} &= -\tfrac{1}{2}G_{46}A_3. \end{aligned} \tag{24}$$

It is evident that, T_0-periodic solutions of (14)must satisfy the following conditions of periodicity for necessity and sufficiency [23].

$$\begin{aligned} \psi_1 &= p_2(T_0, \varepsilon) - p_2(0, \varepsilon) = 0, \\ \psi_2 &= q_2(T_0, \varepsilon) - q_2(0, \varepsilon) = 0, \\ \psi_3 &= \alpha_2(T_0, \varepsilon) - \alpha_2(0, \varepsilon) = 0, \\ \psi_4 &= \beta_2(T_0, \varepsilon) - \beta_2(0, \varepsilon) = 0, \end{aligned} \tag{25}$$

Here $\psi_d(\ d = 1, 2, 3, 4)$ are treated in terms of $(A_j;\ j = 1, 2, 3), \mu$ and ε . The conditions in (25) that determine $A_j^{(0)}, \mu_0$ and a_j are not mutually exclusive due to the presence of the first integrals in equations (11) [20]. Furthermore, if $A_3 \neq 0$, the third condition is expected to follow directly from the others. It is preferable to treat either $A_j^{(0)}$ or α_0 as a

constant, and express one of the a_d as a function of ε which can be removed when $\varepsilon \to \infty$ [31].

Multiplying conditions (25) by ε and setting the free terms of ε to zero, the required conditions for periodicity of $D_h^{(1)}(\ h = 1, 2, 4)$ are obtained in the form

$$D_h^{(1)}(T_0) = D_h^{(1)}(A_1, A_2, A_3, \mu) = 0. \tag{26}$$

To further understand the previous conditions, we utilize equalities (23) to derive:

$$E_{11} + R_{11} = 0, \qquad E_{21} + R_{21} = 0, \qquad E_{31} + R_{41} = 0. \tag{27}$$

It is evident that if the ratio of the frequencies ρ_1 and ρ_2 equals $2, 1/2, 1$ or -1, the resulting expressions for R_{11}, R_{21} and R_{41} are non-zero, as shown below

$$\begin{aligned}
&i) \quad \text{for} \quad \rho_1\rho_2^{-1} = 2,\\
&R_{11} = -\frac{G_{111}}{2},\\
&R_{21} = \frac{G_{216}}{2},\\
&R_{41} = A_3\left[A_1\left(G_{48} - G_{47}\right) + A_2\left(G_{49} - G_{410}\right)\right]/2.\\
&ii) \quad \text{for} \quad \rho_1\rho_2^{-1} = \frac{1}{2},\\
&R_{11} = -\frac{1}{2}\left[A_2A_3\left(G_{17} - G_{16}\right) - A_1A_3\left(G_{116} + G_{117}\right) - G_{123}\right],\\
&R_{21} = -\frac{A_3}{2}\left[A_1\left(G_{25} - G_{28}\right) + A_2\left(G_{26} - G_{27}\right)\right],\\
&R_{41} = -\frac{G_{44}}{2}.\\
&iii) \quad \text{for} \quad \rho_1\rho_2^{-1} = 1,\\
&R_{11} = -\frac{1}{2}\left[A_2A_3^2\left(G_{113} - G_{112}\right) + \left(G_{111} + G_{122}A_3\right)\right],\\
&R_{21} = -\frac{1}{2}\left[G_{213} - G_{24}A_3 - \left(G_{214} + G_{215}\right)A_1A_3^2\right],\\
&R_{41} = \frac{1}{2}\left[\left(G_{43} - G_{41}\right)A_1 + G_{42}A_2 + G_{415} + \left(G_{417} - G_{418}\right)A_1A_3^2\right].\\
&iv) \quad \text{for} \quad \rho_1\rho_2^{-1} = -1,\\
&R_{11} = \frac{G_{122}A_3}{2},\\
&R_{21} = -\frac{G_{24}A_3}{2},\\
&R_{41} = \frac{1}{2}\left[A_1\left(G_{41} - G_{43}\right) - G_{42}A_2\right].
\end{aligned} \tag{28}$$

Assuming $A_j^{(0)}(\ j = 1, 2, 3)$ and μ_0 satisfy (27), we consider Jacobi's matrices of $D_h(T_0)(\ h = 1, 2, 4)$ in terms of A_j and compute both of μ for $A_j = A_j^{(0)}, \mu = \mu_0$, and

ψ_d in terms of a_d vanishes at $\varepsilon \to \infty$ .Computing the second matrix independently of ε . Allowing us to substitute $\varepsilon \to \infty$. Since A_j, μ and a_d are carried out in the solutions as related sums, the resulting matrices are identical and can be denoted by J . The solutions of (25) establish a specific case in which periodic solutions exist.

4. The scenario of irrational frequencies

This section explores the periodic solutions of the investigated problem when the ratio of ρ_1 to ρ_2 is irrational. Notably, these solutions arise when $A_1^{(0)} = A_2^{(0)} = E_{21} = E_{31} = 0,\ E_{11} \neq 0,\ A_3^{(0)}\Gamma_{53} \neq 0$ (where A_3 is an arbitrary quantity) [16], J has a third rank, and

$$\mu_0 = \frac{1}{4\rho_2}\{\Gamma_{85} + \Gamma_{78} - 2(\Gamma_{61} + \Gamma_{63}A_3^{(0)2}) + \frac{\acute{\lambda_2} r_{10}}{\rho_2}[\delta(\Gamma_{65} - 2\Gamma_{68}) + (1 + \chi\delta)\Gamma_{58}\} \tag{29}$$

are met, and equalities (25) have solutions expressed as power series in terms of the large parameter a_1, a_2 and a_4 where a_3 can be set to zero. These solutions approach zero as ε tends to infinity.

Based on the above, the periodicity conditions are expressed as follows

$$\begin{gathered} a_1(\cos\rho_1 T_0 - 1) + a_2 \sin\rho_1 T_0 + \varepsilon^1 D_1^{(1)}(T_0) + ... = 0, \\ -a_1 \sin\rho_1 T_0 + a_2(\cos\rho_1 T_0 - 1) + \varepsilon^1 D_2^{(1)}(T_0) + ... = 0, \\ D_4^{(1)}(T_0) + ... = 0. \end{gathered} \tag{30}$$

According to (29), the unperturbed solutions $p_{20}, q_{20}, \alpha_{20}$ and β_{20} have the forms

$$\begin{aligned} p_2(T,0) &= 0, \\ q_2(T,0) &= -\frac{\acute{\lambda_2} r_{10}(1 + \chi\delta)}{\rho_1}, \\ \alpha_2(T,0) &= A_3^{(0)} \cos\rho_2 T, \\ \beta_2(T,0) &= -A_3^{(0)} \sin\rho_2 T - \frac{\delta\acute{\lambda_2} r_{10}}{\rho_1}. \end{aligned} \tag{31}$$

Based on the area integral in (5) and the conditions (15), we obtain

$$\begin{gathered} A_3^{(0)} = \tfrac{1}{2}G_1^{-1}[-G_2 \pm (G_2^2 + 4G_1G_3)^{1/2}]; \\ G_1 \neq 0, \quad (G_2^2 + 4G_1G_3) > 0. \end{gathered} \tag{32}$$

Here $G_j (j = 1, 2, 3)$ are dependently on of $h, \beta, p_{20}, q_{20}, \alpha_{20}$ and β_{20} which can be determined. Utilizing (29) and (30), a_1 and a_2 are obtained in the forms

$$\begin{aligned}
4\varepsilon a_1 &= -T_0 A_3^{(0)}\{(2\csc^2\tfrac{\rho_1}{2}T_0-1)[\Gamma_{48}+\Gamma_{35}+\tfrac{\acute{\lambda_2}r_{10}}{\rho_1}(\delta\Gamma_{25}-(1+\chi\delta)\\
&\times\Gamma_{15})]+2A_3^{(0)}[\Gamma_{45}+\tfrac{\delta\acute{\lambda_2}r_{10}}{\rho_2}\Gamma_{28}-(1+\tfrac{2\acute{\lambda_2}r_{10}}{\rho_1}(1+\chi\delta)\Gamma_{18})]\}+....,\\
4\varepsilon a_2 &= -T_0 A_3^{(0)}\{(\cot\tfrac{\rho_1}{2}T_0)[\Gamma_{48}+\Gamma_{35}+\tfrac{\acute{\lambda_2}r_{10}}{\rho_1}(\delta\Gamma_{25}-(1+\chi\delta)\Gamma_{15})]\\
&+2A_3^{(0)}[\Gamma_{45}+\tfrac{\delta\acute{\lambda_2}r_{10}}{\rho_2}\Gamma_{28}-(1+\tfrac{2\acute{\lambda_2}r_{10}}{\rho_1}(1+\chi\delta)\Gamma_{18})]\}+.....
\end{aligned}\tag{33}$$

It is worth noting that, the form of a_4 is of order $O(\varepsilon^{-2})$.

Utilizing (3), (6), (9), (14), (22), (23), (29), and (33), the desired solutions are expressed as power series of ε^{-1} in the following forms

$$\begin{aligned}
p &= \varepsilon^{-1/2}n^{-1}[d_1+\chi A_3^{(0)}\cos(\rho_2 n^{-1}t)]+\varepsilon^{-3/2}n^{-1}\{\tfrac{\chi}{2\rho_2}[2(\Gamma_{81}+\Gamma_{83})-\Gamma_{65}A_3^{(0)2}]\\
&+\tfrac{1}{2\rho_1}[2\Gamma_{41}-\Gamma_{27}-\Gamma_{18}+(2\Gamma_{43}-\Gamma_{25})A_3^{(0)2}]+\{\tfrac{\chi t}{2n}A_3^{(0)}[\Gamma_{88}-\Gamma_{75}+\tfrac{\acute{\lambda_2}r_{10}}{\rho_2}\\
&\times(\delta\Gamma_{65}-(1+\delta\chi)\Gamma_{55})]-\tfrac{\chi}{2\rho_2}[2\Gamma_{81}+(2\Gamma_{83}-\Gamma_{65})A_3^{(0)2}]-\tfrac{\chi}{6\rho_2}\Gamma_{65}A_3^{(0)2}\}\\
&\times\cos(\rho_2 n^{-1}t)+\{-\tfrac{\chi}{2\rho_2}A_3^{(0)2}[\Gamma_{88}-\Gamma_{75}+\tfrac{\acute{\lambda_2}r_{10}}{\rho_2}(\delta\Gamma_{65}-(1+\chi\delta)\Gamma_{55})]\\
&+\tfrac{\chi t}{2n}A_3^{(0)}[-2(\Gamma_{61}+\Gamma_{63}A_3^{(0)2})]+\Gamma_{85}+\Gamma_{75}-2\rho_2\mu_0-\tfrac{\acute{\lambda_2}r_{10}}{\rho_2}(\delta\Gamma_{68}-(1+\chi\delta)\\
&\times\Gamma_{58})+\tfrac{\chi}{\rho_2}\Gamma_{68}A_3^{(0)2}]\}\sin(\rho_2 n^{-1})+\{-\tfrac{T_0}{4}A_3^{(0)}(2\csc^2\tfrac{\rho_1}{2}T_0-1)[\Gamma_{48}+\Gamma_{35}\\
&+\tfrac{\acute{\lambda_2}r_{10}}{\rho_1}(\delta\Gamma_{25}-(1+\chi\delta)\Gamma_{15})]-[\tfrac{1}{2\rho_1}[2\Gamma_{41}-\Gamma_{27}-\Gamma_{18}+(2\Gamma_{43}-\Gamma_{25})A_3^{(0)2}]\\
&+\tfrac{t}{2n}\Gamma_{46}A_3^{(0)}]+\tfrac{T_0}{2}A_3^{(0)2}[\Gamma_{45}-\Gamma_{18}+\tfrac{\acute{\lambda_2}r_{10}}{\rho_1}(\delta\Gamma_{28}-2(1+\chi\delta)\Gamma_{18})]\}\\
&\times\cos(\rho_1 n^{-1}t)+\{\tfrac{1}{4}[\tfrac{2}{\rho_1}-T_0A_3^{(0)}(\cot\tfrac{\rho_1}{2}T_0)[\Gamma_{48}+\Gamma_{35}+\tfrac{\acute{\lambda_2}r_{10}}{\rho_1}(\delta\Gamma_{28}\\
&-(1+\chi\delta)\Gamma_{15})]+\tfrac{1}{2}A_3^{(0)2}T_0[\Gamma_{45}+\tfrac{\delta\acute{\lambda_2}r_{10}}{\rho_2}\Gamma_{28}-(1+\tfrac{2\acute{\lambda_2}r_{10}}{\rho_1}(1+\chi\delta)\Gamma_{18})]\\
&+\tfrac{1}{2}A_3^{(0)2}T_0[\Gamma_{45}-\Gamma_{18}+\tfrac{\acute{\lambda_2}r_{10}}{\rho_1}(\delta\Gamma_{28}-2(1+\chi\delta)\Gamma_{18})]-\tfrac{t}{6n\rho_1}A_3^{(0)2}T_0\Gamma_{28}\\
&+A_3^{(0)}T_0[\Gamma_{45}-\Gamma_{38}-\tfrac{\acute{\lambda_2}r_{10}}{\rho_1}(\delta\Gamma_{28}-(1+\chi\delta))]\}\sin(\rho_1 n^{-1}t)+\tfrac{\chi}{6\rho_2}[A_3^{(0)2}\Gamma_{65}\\
&\times\cos(2\rho_2 n^{-1}t)-3\Gamma_{68}\sin(2\rho_2 n^{-1}t)]+\tfrac{\chi}{6\rho_1}A_3^{(0)2}\Gamma_{28}\sin(2\rho_1 n^{-1}t)\}+....,
\end{aligned}$$

$$q = -\varepsilon^{-1/2}n^{-1}\{\chi[\tfrac{\delta\acute{\lambda_2}r_{10}}{\rho_2} + A_3^{(0)}\sin(\rho_2 n^{-1}t)] - \tfrac{\acute{\lambda_2}r_{10}}{\rho_1}(1+\chi\delta)\} + \varepsilon^{-3/2}n^{-1}\{-\tfrac{1}{\rho_2}$$
$$\{\chi[2\delta\acute{\lambda_2}r_{10}\mu_0 - \Gamma_{71} + \tfrac{\acute{\lambda_2}r_{10}}{\rho_2}[\delta(\Gamma_{61}+\Gamma_{63}A_3^{(0)2}) - (1+\chi\delta)(\Gamma_{51}+\Gamma_{53}A_3^{(0)2})]$$
$$+\tfrac{1}{2}A_3^{(0)2}(\Gamma_{68}-2\Gamma_{73})] + \tfrac{1}{\rho_1}[-2(1+\chi\delta)\acute{\lambda_2}r_{10}\mu_0 - \Gamma_{31} + \tfrac{1}{2}A_3^{(0)2}(\Gamma_{28}-2\Gamma_{33})]$$
$$-\tfrac{\acute{\lambda_2}r_{10}}{\rho_1}[\delta(\Gamma_{21}+\Gamma_{23}A_3^{(0)2}) - (1+\chi\delta)(\Gamma_{11}+\Gamma_{13}A_3^{(0)2})]\} + \chi\{-\tfrac{t}{2n}A_3^{(0)}[\Gamma_{85}+\Gamma_{78}$$
$$-4\rho_2\mu_0 - 2(\Gamma_{61}+\Gamma_{63}A_3^{(0)2}) + \tfrac{\acute{\lambda_2}r_{10}}{\rho_2}[\delta(\Gamma_{65}-2\Gamma_{68}) + (1+\chi\delta)\Gamma_{58}]] + \tfrac{1}{\rho_2}[\delta\acute{\lambda_2}r_{10}\mu_0$$
$$-(\Gamma_{71}+\Gamma_{73}A_3^{(0)2}) + \tfrac{\acute{\lambda_2}r_{10}}{\rho_2}[\delta(\Gamma_{61}+\Gamma_{63}A_3^{(0)2}) - (1+\chi\delta)(\Gamma_{51}+\Gamma_{53}A_3^{(0)2})]]\}$$
$$\times\cos(\rho_2 n^{-1}t) + \tfrac{\chi}{2}A_3^{(0)}\{\tfrac{t}{n}[\Gamma_{88}-\Gamma_{75} + \tfrac{\acute{\lambda_2}r_{10}}{\rho_2}[\delta\Gamma_{65} - (1+\chi\delta)\Gamma_{55}]] - \tfrac{2}{\rho_2}\Gamma_{65}A_3^{(0)}$$
$$+\tfrac{1}{\rho_2}[\Gamma_{85}+\Gamma_{78}-4\rho_2\mu_0 - 2(\Gamma_{61}+\Gamma_{63}A_3^{(0)2}) + \tfrac{\acute{\lambda_2}r_{10}}{\rho_2}[\delta(\Gamma_{65}-2\Gamma_{68}) + (1+\chi\delta)\Gamma_{58}]]\}$$
$$\times\sin(\rho_2 n^{-1}t) + \tfrac{\chi}{2\rho_2}A_3^{(0)2}[\Gamma_{68}\cos(2\rho_2 n^{-1}t) + \Gamma_{65}\sin(2\rho_2 n^{-1}t)] + \tfrac{T_0}{4}A_3^{(0)}\{(2$$
$$\times\csc^2\tfrac{\rho_1}{2}T_0 - 1)[\Gamma_{48}+\Gamma_{35} + \tfrac{\acute{\lambda_2}r_{10}}{\rho_1}(\delta\Gamma_{25} - (1+\chi\delta)\Gamma_{15})] - \tfrac{T_0}{2}A_3^{(0)}[\Gamma_{45}-\Gamma_{18}$$
$$+\tfrac{\acute{\lambda_2}r_{10}}{\rho_1}(\delta\Gamma_{28} - 2(1+\chi\delta)\Gamma_{18})] - \tfrac{1}{2\rho_1}[\Gamma_{18}-\Gamma_{45} + \tfrac{\acute{\lambda_2}r_{10}}{\rho_1}(\delta\Gamma_{28} + 2(1+\chi\delta)\Gamma_{18})]$$
$$-\tfrac{1}{3\rho_1}\Gamma_{25}A_3^{(0)} + \tfrac{t}{2n}[\Gamma_{15}+\Gamma_{18} + \tfrac{\acute{\lambda_2}r_{10}}{\rho_1}(\delta\Gamma_{25} + 2(1+\chi\delta)\Gamma_{15})]\}\sin(2\rho_1 n^{-1}t)$$
$$+\{-\tfrac{T_0}{4}A_3^{(0)}\cot(\tfrac{\rho_1}{2}T_0)[\Gamma_{48}+\Gamma_{35} + \tfrac{\acute{\lambda_2}r_{10}}{\rho_1}(\delta\Gamma_{25} - (1+\chi\delta)\Gamma_{15})] + \tfrac{1}{2}A_3^{(0)2}T_0[\Gamma_{45}$$
$$-\Gamma_{18} + \tfrac{\acute{\lambda_2}r_{10}}{\rho_1}(\delta\Gamma_{28} - 2(1+\chi\delta)\Gamma_{18})] - \tfrac{1}{\rho_2}[-2(1+\chi\delta)\acute{\lambda_2}r_{10}\mu_0 + \tfrac{1}{2}\Gamma_{28}A_3^{(0)2}$$
$$-(\Gamma_{31}+\Gamma_{33}A_3^{(0)2})] - \tfrac{\acute{\lambda_2}r_{10}}{\rho_1}[\delta(\Gamma_{21}+\Gamma_{23}A_3^{(0)2}) - (1+\chi\delta)(\Gamma_{11}+\Gamma_{13}A_3^{(0)2})]$$
$$+\tfrac{t}{2n}A_3^{(0)}[\Gamma_{18}-\Gamma_{45} + \tfrac{\acute{\lambda_2}r_{10}}{\rho_1}(\delta\Gamma_{28} + 2(1+\chi\delta)\Gamma_{18})] + \tfrac{1}{6\rho_1}\Gamma_{28}A_3^{(0)2})\}\cos(\rho_1 n^{-1}t)$$
$$+\tfrac{1}{6\rho_1}A_3^{(0)2}[\Gamma_{25}\sin(2\rho_1 n^{-1}t) - \Gamma_{28}\cos(2\rho_1 n^{-1}t)]\} + ...,$$

$$r = \tfrac{r_0}{n} - \tfrac{\varepsilon^{-1}}{nbr_{10}}A_3^{(0)}\{[(1+\chi\delta)(d_2-1) + \chi d_1](\cos(\rho_2 n^{-1}t) - 1)$$
$$+\tfrac{\acute{\lambda_2}r_{10}}{\rho_1\rho_2}[\delta(\rho_1+\rho_2)[\chi^2 + (1+\chi\delta)^2] + \rho_2\chi]\sin(\rho_2 n^{-1}t)\} + ...,$$

$$\alpha = \varepsilon^{-1/2}[d_2 + (1+\chi\delta)A_3^{(0)}\cos(\rho_2 n^{-1}t)] + \varepsilon^{-3/2}\{\tfrac{(1+\chi\delta)}{2\rho_2}[2\Gamma_{81} + (2\Gamma_{83}-\Gamma_{65})$$
$$\times A_3^{(0)2}] + \tfrac{\delta}{2\rho_1}[2\Gamma_{41} - \Gamma_{27} - \Gamma_{18} + (2\Gamma_{43}-\Gamma_{25})A_3^{(0)2}] + (1+\chi\delta)\{\tfrac{t}{2n}A_3^{(0)}$$
$$\times[\Gamma_{88} - \Gamma_{75} + \tfrac{\acute{\lambda_2}r_{10}}{\rho_2}(\delta\Gamma_{65} - (1+\chi\delta)\Gamma_{55})] - \tfrac{1}{2\rho_2}[2\Gamma_{81} + (2\Gamma_{83}-\Gamma_{65})A_3^{(0)2}]$$
$$-\tfrac{1}{6\rho_2}A_3^{(0)2}\Gamma_{65}\}\cos(\rho_2 n^{-1}t) + (1+\chi\delta)\{-\tfrac{1}{2\rho_2}A_3^{(0)}[\Gamma_{88} - \Gamma_{75} + \tfrac{\acute{\lambda_2}r_{10}}{\rho_2}(\delta\Gamma_{65}$$
$$-(1+\chi\delta)\Gamma_{55})] + \tfrac{t}{2n}A_3^{(0)}[\Gamma_{85}+\Gamma_{78} - 2\rho_2\mu_0 - 2(\Gamma_{61}+\Gamma_{63}A_3^{(0)2} - \tfrac{\acute{\lambda_2}r_{10}}{\rho_2}(\delta\Gamma_{68}$$
$$-(1+\chi\delta)\Gamma_{58})] + \tfrac{1}{\rho_2}A_3^{(0)2}\Gamma_{68}\}\sin(\rho_2 n^{-1}t) + \tfrac{(1+\chi\delta)}{6\rho_2}A_3^{(0)2}[\Gamma_{65}\cos(2\rho_2 n^{-1}t)$$
$$-\Gamma_{68}\sin(\rho_2 n^{-1}t)] - \{\tfrac{T_0\delta}{4}A_3^{(0)}(2\csc^2\tfrac{\rho_1}{2}T_0 - 1)[\Gamma_{48}+\Gamma_{35} + \tfrac{\acute{\lambda_2}r_{10}}{\rho_1}(\delta\Gamma_{25}$$
$$-(1+\chi\delta)\Gamma_{15})] - \tfrac{T_0}{2}A_3^{(0)2}[\Gamma_{45}-\Gamma_{18} + \tfrac{\acute{\lambda_2}r_{10}}{\rho_1}(\delta\Gamma_{28} - 2(1+\chi\delta)\Gamma_{18})] + \tfrac{\delta}{2}[\tfrac{1}{\rho_1}(2\Gamma_{41}$$
$$-\Gamma_{27}-\Gamma_{18}) + \tfrac{1}{\rho_1}(2\Gamma_{43}-\Gamma_{25})A_3^{(0)2} + \tfrac{t}{n}\Gamma_{46}A_3^{(0)}]\}\cos(\rho_1 n^{-1}t) - \delta\{-\tfrac{1}{4}[\tfrac{2}{\rho_1}$$
$$-T_0A_3^{(0)}(\cot\tfrac{\rho_1}{2}T_0)[\Gamma_{48}+\Gamma_{35} + \tfrac{\acute{\lambda_2}r_{10}}{\rho_1}(\delta\Gamma_{25} - (1+\chi\delta)\Gamma_{15})] + \tfrac{1}{2}A_3^{(0)2}T_0[\Gamma_{45}$$
$$-\Gamma_{18} + \tfrac{\acute{\lambda_2}r_{10}}{\rho_1}(\delta\Gamma_{28} - 2(1+\chi\delta)\Gamma_{18})] + \tfrac{t}{6\rho_1}\Gamma_{28}A_3^{(0)2} + A_3^{(0)}[\Gamma_{45} - \Gamma_{38} + \tfrac{\acute{\lambda_2}r_{10}}{\rho_1}$$
$$\times(1+\chi\delta - \delta\Gamma_{28})]\}\sin(\rho_1 n^{-1}t) + \tfrac{\delta}{6\rho_1}A_3^{(0)2}\sin(2\rho_1 n^{-1}t)\} + ...,$$

$$\beta = -\varepsilon^{-1/2}(1+\chi\delta)\{\tfrac{\delta\acute{\lambda_2}r_{10}}{\rho_1\rho_2}(\rho_1+\rho_2)+A_3^{(0)}\sin(\rho_2 n^{-1}t)\}+\varepsilon^{-3/2}\{-\tfrac{(1+\chi\delta)}{2\rho_2}[2\delta\acute{\lambda_2}r_{10}$$
$$\times\mu_0+\tfrac{\acute{\lambda_2}r_{10}}{\rho_2}[\delta(\Gamma_{61}+\Gamma_{63}A_3^{(0)2})-(1+\chi\delta)(\Gamma_{51}+\Gamma_{53}A_3^{(0)2})]-(\Gamma_{71}+\Gamma_{73}$$
$$\times A_3^{(0)2})+\tfrac{1}{2}A_3^{(0)2}\Gamma_{68}]+\tfrac{\delta}{\rho_1}[-2(1+\chi\delta)\acute{\lambda_2}r_{10}\mu_0+\tfrac{1}{2}A_3^{(0)2}(\Gamma_{28}-2\Gamma_{33})-\Gamma_{31}$$
$$-\tfrac{\acute{\lambda_2}r_{10}}{\rho_1}[\delta(\Gamma_{21}+\Gamma_{23}A_3^{(0)2})-(1+\chi\delta)(\Gamma_{11}+\Gamma_{13}A_3^{(0)})]]+(1+\chi\delta)\{-\tfrac{t}{2n}\}[\Gamma_{85}$$
$$+\Gamma_{78}-4\rho_2\mu_0+\tfrac{\acute{\lambda_2}r_{10}}{\rho_2}[\delta(\Gamma_{65}-2\Gamma_{68})+(1+\chi\delta)\Gamma_{58}]]+\tfrac{1}{\rho_2}[2\delta\acute{\lambda_2}r_{10}\mu_0-\Gamma_{71}$$
$$-\Gamma_{73}A_3^{(0)2}+\tfrac{\lambda_2 r_{10}}{\rho_2}[\delta(\Gamma_{61}-\Gamma_{63}A_3^{(0)2})-(1+\chi\delta)(\Gamma_{51}+\Gamma_{53}A_3^{(0)2})]]\}$$
$$\times\cos(\rho_2 n^{-1}t)+(1+\chi\delta)\{\tfrac{t}{2n}A_3^{(0)}[\Gamma_{88}-\Gamma_{75}+\tfrac{\acute{\lambda_2}r_{10}}{\rho_2}[\delta\Gamma_{65}-(1+\chi\delta)\Gamma_{55}]]-\tfrac{1}{\rho_2}$$
$$\times\Gamma_{65}A_3^{(0)2}+\tfrac{1}{2\rho_2}A_3^{(0)}[\Gamma_{85}+\Gamma_{78}-4\rho_2\mu_0+\tfrac{\acute{\lambda_2}r_{10}}{\rho_2}[\delta(\Gamma_{65}-2\Gamma_{68})+(1+\chi\delta)\Gamma_{58}$$
$$-2(\Gamma_{61}+\Gamma_{63}A_3^{(0)2})]]\}\sin(\rho_2 n^{-1}t)+\tfrac{(1+\chi\delta)}{2\rho_2}A_3^{(0)2}[\Gamma_{68}\cos(2\rho_2 n^{-1}t)+\Gamma_{65}$$
$$\times\sin(2\rho_2 n^{-1}t)]+\delta\{\tfrac{T_0}{4}A_3^{(0)}(2\csc^2\tfrac{\rho_1}{2}T_0-1)[\Gamma_{48}+\Gamma_{35}+\tfrac{\acute{\lambda_2}r_{10}}{\rho_1}(\delta\Gamma_{25}-(1+\chi\delta)\Gamma_{15})]$$
$$+\tfrac{T_0}{2}A_3^{(0)2}[\Gamma_{18}-\Gamma_{45}-\tfrac{\acute{\lambda_2}r_{10}}{\rho_1}(\delta\Gamma_{28}-2(1+\chi\delta)\Gamma_{18})]-\tfrac{1}{3\rho_1}A_3^{(0)2}\Gamma_{25}-\tfrac{1}{2\rho_1}A_3^{(0)}[\Gamma_{18}$$
$$-\Gamma_{45}+\tfrac{\acute{\lambda_2}r_{10}}{\rho_1}(\delta\Gamma_{28}+2(1+\chi\delta)\Gamma_{18})]+\tfrac{t}{2n}A_3^{(0)}[\Gamma_{18}+\Gamma_{15}+\tfrac{\acute{\lambda_2}r_{10}}{\rho_1}(\delta\Gamma_{25}$$
$$+2(1+\chi\delta)\Gamma_{15})]\}\sin(\rho_1 n^{-1}t)+\delta\{-\tfrac{T_0A_3^{(0)}}{4}(\cot\tfrac{\rho_1}{2}T_0)[\Gamma_{48}+\Gamma_{35}+\tfrac{\acute{\lambda_2}r_{10}}{\rho_1}(\delta\Gamma_{25}-(1+\chi\delta)\Gamma_{15})]$$
$$+\tfrac{1}{2}A_3^{(0)2}T_0[\Gamma_{45}-\Gamma_{18}+\tfrac{\acute{\lambda_2}r_{10}}{\rho_1}(\delta\Gamma_{28}-2(1+\chi\delta)\Gamma_{18})]+\tfrac{1}{\rho_1}[2\acute{\lambda_2}r_{10}(1+\chi\delta)\mu_0-\tfrac{1}{2}\Gamma_{28}$$
$$\times A_3^{(0)2}+\Gamma_{31}+\Gamma_{33}A_3^{(0)2}+\tfrac{\acute{\lambda_2}r_{10}}{\rho_1}[\delta(\Gamma_{21}+\Gamma_{23}A_3^{(0)2})-(1+\chi\delta)(\Gamma_{11}+\Gamma_{13}A_3^{(0)2})]]+\tfrac{t}{2n}$$
$$\times A_3^{(0)}[\Gamma_{18}-\Gamma_{45}+\tfrac{\acute{\lambda_2}r_{10}}{\rho_1}(\delta\Gamma_{28}+2(1+\chi\delta)\Gamma_{18})]+\tfrac{1}{6\rho_1}\Gamma_{28}A_3^{(0)2}\}\cos(\rho_1 n^{-1}t)$$
$$+\tfrac{\delta}{6\rho_1}A_3^{(0)2}[\Gamma_{25}\sin(2\rho_1 n^{-1}t)-\Gamma_{28}\cos(2\rho_1 n^{-1}t)]\}+...,$$

$$\gamma = 1-\tfrac{1}{2}\varepsilon^{-1}\{(1+\chi\delta)^2[\tfrac{\delta\acute{\lambda_2}r_{10}}{\rho_2}+A_3^{(0)}\sin(\rho_2 n^{-1}t)]^2+[d_2+(1+\chi\delta)A_3^{(0)}\cos(\rho_2 n^{-1}t)]^2\}+....,$$

$$\mu_0 = \tfrac{1}{4\rho_2}\{\Gamma_{85}+\Gamma_{78}-2(\Gamma_{61}+\Gamma_{63}A_3^{(0)2})+\tfrac{\acute{\lambda_2}r_{10}}{\rho_2}[\delta(\Gamma_{65}-2\Gamma_{68})+(1+\chi\delta)\Gamma_{58}]\},$$

$$T_0 = 2\pi\rho_2^{-1}. \tag{34}$$

As a result of the fact that the rotatory motion of a RB in 3D is governed by nonlinear differential equations, it is frequently difficult or even impossible to obtain exact solutions in many practical scenarios [1, 3, 7]. Therefore, the AS play an essential role in comprehending, predicting, and optimizing the rotational behavior of such systems. The following are the primary reasons why that are important:

This problem is governed by Euler's equations [49], which are highly nonlinear due to the interdependence of angular velocities and moments of inertia. The nonlinear nature of the problem makes finding exact solutions for arbitrary initial conditions or external forces nearly impossible, necessitating the use of approximate methods such as perturbation techniques, numerical simulations, or asymptotic analysis [50].

The use of the AS make it possible to do computations in an effective manner, which makes them suited for real-time applications in which exact results are not feasible. For the

purpose of providing feedback control, numerous control systems in the fields of robotics, aircraft, and navigation require extremely quick and real-time estimates of rotational motion [51].

By analyzing small perturbations, AS facilitate the assessment of rotational stability, enabling engineers to predict whether a system will sustain stable motion or shift into chaotic behavior. The evolution of rotational motion in RBs over extended periods, including effects like precession and nutation, can be computationally demanding [52]. The AS provide an efficient alternative for studying these dynamics. Rotating systems are often susceptible to resonance, where periodic external forces intensify oscillations. Approximate approaches like multiple-scales method and averaging one [50] help detect critical frequencies and optimize system design to prevent instability.

RBs in engineering applications frequently undergo compound rotational motion, including spinning and chaotic dynamics. AS provide computationally efficient models that retain essential physical insights. Numerical simulations, including finite element analysis and Runge-Kutta integration, provide precise results but are computationally demanding [53]. Approximate analytical methods offer initial insights, serving as a foundation for further refinement using computational techniques. As benchmark models, the AS help validate experimental data, allowing researchers to compare predictions, refine models, and detect discrepancies.

Therefore, the nonlinear nature of the governing EOM makes obtaining AS RB rotation essential. These approximations enable real-time computation, stability analysis, and long-term motion prediction, providing practical benefits across aerospace, robotics, biomechanics, and structural engineering.

5. Euler's angles and interpretation of motion

This section is dedicated to analyzing Eulerâ€™s angles for the motion of the given body within the context of the obtained solutions, offering a geometrical interpretation of motion through at any moment. These angles are crucial for determining the orientation of a RB in 3D space. They offer a structured approach to defining a RBâ€™s orientation in 3D space through three sequential rotations relative to a fixed reference frame, ensuring a clear and systematic representation of rotation [54]. With only three parameters, these angles provide a simpler and more computationally efficient alternative to rotation matrices and quaternions, making them easier to interpret in engineering contexts.

Euler angles are essential in aerospace for defining the orientation of aircraft, satellites, and spacecraft, supporting navigation, attitude control, and stabilization. In robotics, they facilitate precise positioning and motion planning for robotic arms and autonomous systems [55]. They are fundamental to RB dynamics, aiding in the formulation and solution of Eulerâ€™s EOM. They offer a simplified representation of angular velocity and acceleration, enhancing mechanical and aerospace studies.

Numerous sensors, such gyroscopes are useful for motion tracking and control systems in the real world because they measure orientation in terms of these angles. For smooth and organic object orientation control, Euler angles are frequently utilized in computer graphics

and animation. Additionally, they are employed in simulation and game development physics engines. They provide a structured approach to analyzing rotational behaviors, including precession, nutation, and spin, which are essential in planetary motion, satellite dynamics, and gyroscopic systems [55].

A fundamental approach involves applying the expressions for Eulerâ€™s angles θ, ψ and ϕ as in [1].

$$\begin{aligned} \theta &= \cos^{-1}\gamma, \\ \dot{\psi} &= \frac{p\alpha + q\beta}{1-\gamma^2}, \\ \dot{\phi} &= r - \dot{\psi}\cos\theta, \\ \phi_0 &= \tan^{-1}\left(\frac{\alpha_0}{\beta_0}\right); \quad \left(\dot{} \equiv \frac{d}{dt}\right). \end{aligned} \tag{35}$$

Substituting the achieved solutions (34) into expressions (35) to obtain θ, ψ and ϕ as follows

$$\begin{aligned} \theta = \theta_0 + \varepsilon^{-1}(1+\chi\delta)A_3^{(0)}\csc\theta_0 \Big[& \tfrac{\delta\lambda_2' r_{10}}{\rho_2}(1+\chi\delta)\left[\sin\left(\rho_2 n^{-1}(t+\chi)\right) - \sin\left(\rho_2 n^{-1}\chi\right)\right] \\ & + d_2\left[\cos\left(\rho_2 n^{-1}(t+\chi)\right) - \cos\left(\rho_2 n^{-1}\chi\right)\right]\Big] + \cdots, \end{aligned}$$

$$\begin{aligned} \psi = \psi_0 + \varepsilon n^{-1}\csc^2\theta_0 \Big\{ & d_1 d_2 + (1+\chi\delta)\left[\tfrac{\delta(\acute{\lambda_2} r_{10})^2}{\rho_1^2\rho_2}(\rho_1+\rho_2)\left[\tfrac{\delta\chi}{\rho_2}(\rho_1+\rho_2)+1\right] + \chi A_3^{(0)2}\right] t \\ & + \tfrac{nA_3^{(0)}}{\rho_2}\left[d_2\chi + d_1(1+\chi\delta)\right]\sin\left(\rho_2 n^{-1}t\right) - \tfrac{n\acute{\lambda_2} r_{10}}{\rho_1\rho_2}(1+\chi\delta)A_3^{(0)}\left[\tfrac{2\chi\delta}{\rho_2}(\rho_1+\rho_2)+1\right] \\ & \times\left(\cos\left(\rho_2 n^{-1}t\right) - 1\right)\Big\} + \cdots, \end{aligned}$$

$$\begin{aligned} \phi = \phi_0 + \tfrac{r_{10}}{n}t - \tfrac{\varepsilon^{-1}}{n}\Big\{ & \tfrac{\varepsilon A_3^{(0)}}{nbr_{10}}\left[(1+\chi\delta)(d_2-1) + \chi d_1\right]\left[\tfrac{n}{\rho_2}\sin\left(\rho_2 n^{-1}t\right) - t\right] \\ & - \tfrac{n\acute{\lambda_2} r_{10}}{\rho_1\rho_2^2}\left[\delta(\rho_1+\rho_2)\left(\chi^2 + (1+\chi\delta)^2\right) + \rho_2\chi\right]\left(\cos\left(\rho_2 n^{-1}t\right) - 1\right)\Big\} \\ + \csc^2\theta_0\cos\theta_0\Big\{ & d_1^2 + (1+\chi\delta)\left[\tfrac{\delta(\acute{\lambda_2} r_{10})^2}{\rho_1^2\rho_2}(\rho_1+\rho_2)\left[\tfrac{\chi\delta}{\rho_2}(\rho_1+\rho_2)+1\right] + \chi A_3^{(0)2}\right] t \\ & + \tfrac{nA_3^{(0)}}{\rho_2}\left[d_2\chi + d_1(1+\chi\delta)\right]\sin\left(\rho_2 n^{-1}t\right) - \tfrac{n\acute{\lambda_2} r_{10}}{\rho_1\rho_2}(1+\chi\delta)A_3^{(0)}\left[\tfrac{2\chi\delta}{\rho_2}(\rho_1+\rho_2)+1\right] \\ & \times\left(\cos\left(\rho_2 n^{-1}t\right) - 1\right)\Big\} + \cdots \end{aligned} \tag{36}$$

where

$$\phi_0 = \frac{\pi}{2} - \rho_1 n^{-1}\chi.$$

Equation (36) clearly shows that the Euler angles of the examined motion are dependent on the arbitrary constants θ_0, ψ_0 and r_0.

6. Evaluation of the outcomes

This section primarily focuses on presenting and analyzing the results outlined in (34) and (36) using the graphical representations of the obtained solutions to highlight the influence of various parameters on the body's motion over time and to emphasize the significance of the GM. Accordingly, the following data are considered

$$I_1 = I_2 = 10^3 kg.m^2, \quad I_3 = 800 kg.m^2, \quad \varepsilon = 1000, \quad x_G = 1m,$$
$$M = 50kg, \quad g = 9.8 kg.s^{-2}, \quad r_0 = 1.2, \quad \theta_0 = 10^{-10}$$
$$\lambda_2, \lambda_3 = (10, 30, 60) kg.m^2.s^{-1}.$$

Fig.2, and Fig.4 illustrate the temporal progression of the outcomes obtained from the system of equations (34) under different values of λ_2 and λ_3 , respectively. Meanwhile, the corresponding phase plane diagrams, generated using the same parameter settings, are depicted in Figs. Fig.3, and Fig.5. These visualizations are derived from the data previously presented.

Fig.2 illustrates the variation of the time-dependent functions p, q, r, α, β and γ when λ_2 has distinct values of $(10, 30, 60) kg.m^2.s^{-1}$. Certain sections of this figure are computed at $\lambda_3 = 10 kg.m^2.s^{-1}$.

The main purpose of the curves in Fig.2 is to examine the positive effects of the selected values of the gyro's second projection $\lambda_2 = (10, 30, 60) kg.m^2.s^{-1}$ on the body's behavior. As anticipated, periodic waves appear in certain portions of this figure. The solutions p and α show only small variations with different values of λ_2 , as demonstrated in Fig.2 in a and d respectively. This behavior arises from the governing equations, which either do not explicitly depend on it or encompass it within a bracket alongside λ_2. However, the other potions (b), (c), (e), and (f) are significantly influenced by changes in values. Notably, the wave amplitudes increase as increases, as shown in Fig.2 in e and f respectively. Additionally, neither the number of fluctuations nor the wavelength of the waves undergoes any change.

The body's steady behavior is depicted through the phase plane graphs of the obtained solutions when $\lambda_2 (= 10, 30, 60) kg.m^2.s^{-1}$, as shown in Fig.3. The plotted curves represent the solutions via their first derivatives, with time being excluded. Notably, symmetric closed curves emerge, highlighting and validating the stability behavior of the body's motion.

Curves in Fig.4 show how the solutions p, q, r, α, β and γ change for distinct values of λ_3 (e. g.$10, 30$ and 60). These solutions are affected by variations in λ_3 , producing periodic waves with distinct amplitudes, as shown in parts of Fig.3. As values increase, the amplitudes of these waves decrease. The plots of phase plane of these waves, shown in portions of Fig.5, further demonstrate the stable nature of the results. The results indicate that the solutions maintain stability, without any chaotic characteristics.

It is evident that Euler's angles θ, ψ and ϕ significantly contribute to determining the orientation of the RB. To investigate this aspect, relations (37) are plotted in Figs.6 and Figs.7, considering the previously provided data to analyze the impact of different values of λ_2, and λ_3 on the body's dynamic behavior. Notably, Figs.6 are plotted at

$\lambda_2(=10,30,60)kg.m^2.s^{-1}$ and $\lambda_3 = 10$ respectively, while Figs. (7) are computed at $\lambda_2 = 10$ and,$\lambda_3(=10,30,60)kg.m^2.s^{-1}$ respectively.

Notably, the behavior of the nutation angle θ positively influences λ_3 as it increases over time, as illustrated in Fig.6 and Fig.7, in panel a . This effect arises from the first approximate term, which depends on ρ_1, ρ_2, χ and δ . It is apparent that the wave amplitude grows moderately, while the oscillation count remains constant. On the other side, the behavior of the waves representing the precession angle ψ changes gradually as λ_2 increases, as shown in panel b of Fig.6 and Fig.7. However, there is no noticeable variation in the waves describing the self-rotation angle ϕ , as seen in panel c of Fig.6 and panel c of Fig.7. The negative values of ϕ arise due to the difference between the first and second terms in the equation, where the second term is significantly larger than the first. Additionally, it should be noted that the inaccuracy in ϕ plays a crucial role in these results.

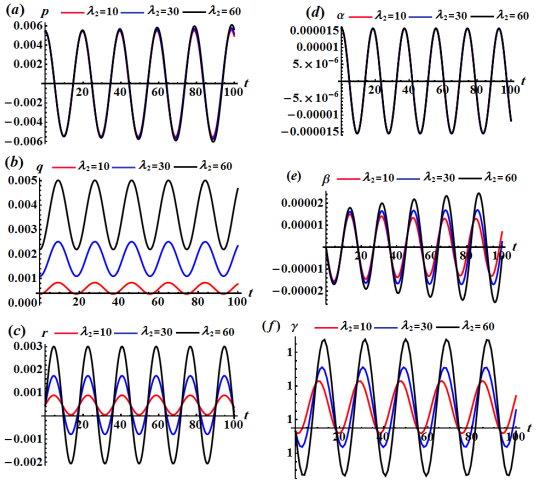

Figure 2: Presents the variations of $p(t), q(t), r(t), \alpha(t), \beta(t)$ and $\gamma(t)$ when $\lambda_2 = (10, 30, 60)\,\mathrm{kg}\cdot\mathrm{m}^2\cdot\mathrm{s}^{-1}$ and $\lambda_3 = 10$ are considered.

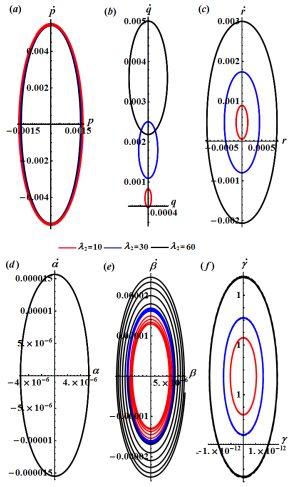

Figure 3: Depicts the phase plane representations of time dependent functions in Fig.2.

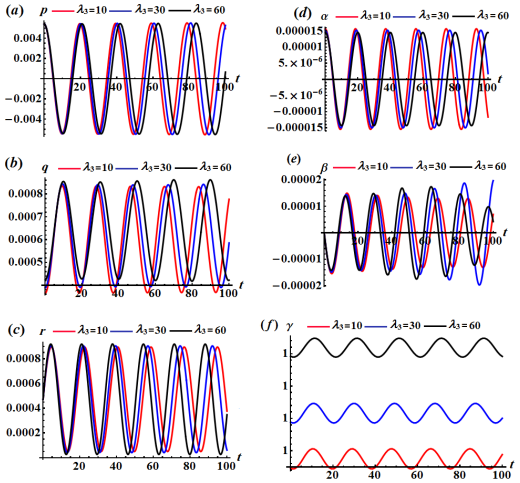

Figure 4: Shows the variation of $p(t), q(t), r(t), \alpha(t), \beta(t)$ and $\gamma(t)$ when $\lambda_3 = (10, 30, 60) kg.m^2.s^{-1}$ and $\lambda_2 = 10$.

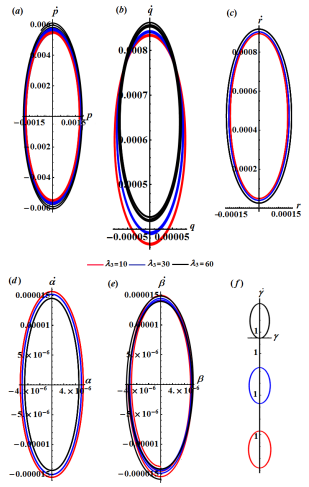

Figure 5: Reveals the phase plane plots of time dependent functions in Fig.4.

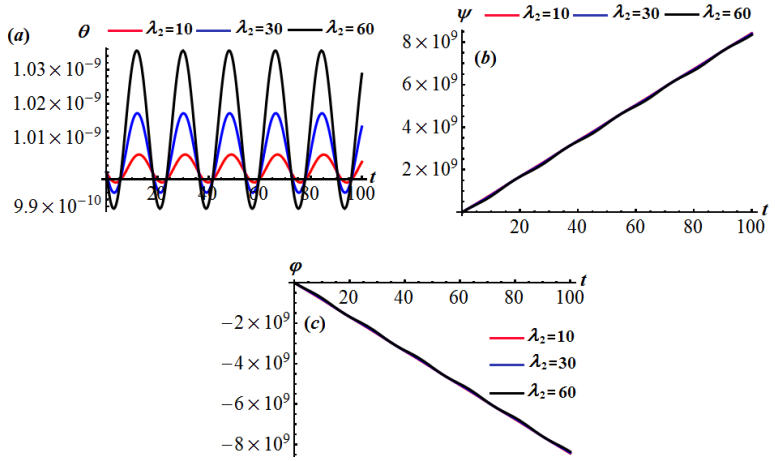

Figure 6: Presents the temporal histories of: (a) θ, (b) ψ, and (c) ϕ at $\lambda_2(= 10, 30, 60)$ and $\lambda_3 = 10$.

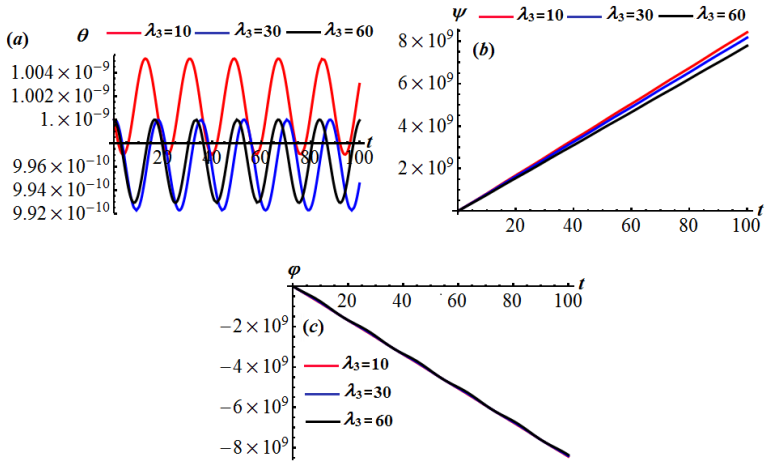

Figure 7: Shows the time histories of the angles (a) θ, (b) ψ, and (c) ϕ when $\lambda_3(= 10, 30, 60)$ and $\lambda_2 = 10$ are consided.

7. Conclusion

This work analyzes the three-dimensional motion of a new RB according to Lagrange's gyroscope model, considering a new condition by giving the body a very much displacement of the center of mass from the axis of dynamic symmetry. The body is influenced by a GM along the main inertia axes and a NFF. The governing EOM and their first integrals are reformulated as a nonlinear dynamical system of four first-order DEs, which are solved via the LPA. Advanced computational tools are employed to analyze the solutions and visualize the influence of varying applied moments and NFF on the body's motion. These solutions extend and generalize previous findings by Elfimov [26], which considered the absence of external moments and forces, and by Amer [16], which examined the case of a uniform field. The stability of the obtained solutions is evaluated using computational methods, generating diagrams of the phase plane which confirm the motion remains free of chaotic behavior. Additionally, geometric interpretations are conducted to determine the body's orientation over time, utilizing Euler's angles. Time-histories plots of these angles further illustrate the effects of different physical parameters on motion. This research is highly relevant due to its wide-ranging applications in celestial mechanics, physics, and gyroscopic systems, offering valuable insights into the dynamics of rigid bodies subjected to complex force interactions. This study is expected to significantly impact the aerospace industry by enhancing our understanding of rotational motion and celestial dynamics, with direct applications in the design and operation of spacecraft, satellites, and other space vehicles.

Authors' Statements

- **T. S. Amer**: Investigation, Methodology, Data curation, Conceptualization, Validation, Reviewing and Editing.
- **A. I. Ismail**: Methodology, Data curation, Conceptualization, Validation, Reviewing and Editing.
- **W. S. Amer**: Conceptualization, Resources, Formal Analysis, Validation, Visualization, and Reviewing.
- **H. F. El-Kafly**: Resources, Methodology, Conceptualization, Validation, Formal Analysis, Visualization, and Reviewing.

Conflict of Interest

The authors declare that they have no conflict of interest.

Funding Acknowledgements

The author extends their appreciation to Umm-Alqura University, Saudi Arabia for funding this research work through grant number: 25UQU4240002GSSR06

Data Availability

Data sharing not applicable to this article as no datasets were generated or analyzed during the current study.

References

[1] Eugene Leimanis. *The General Problem of the Motion of Coupled Rigid Bodies about a Fixed Point*, volume 7. Springer Science & Business Media, 2013.

[2] H. M. Yehia and A. A. Elmandouh. New conditional integrable cases of motion of a rigid body with kovalevskaya's configuration. *Journal of Physics A: Mathematical and Theoretical*, 44(8), 2011.

[3] A. I. Ismail and T. S. Amer. A necessary and sufficient condition for solving a rigid body problem. *Technische Mechanik*, 31(1):50–57, 2011.

[4] Iu. A. Arkhangel'skii. On the algebraic integrals in the problem of motion of a rigid body in a newtonian field of force. *Journal of Applied Mathematics and Mechanics*, 27(1):247–254, 1963.

[5] Hamad M. Yehia. Rigid body dynamics. *Advances in Mechanics and Mathematics*, 2022.

[6] A. A. Elmandouh. New integrable problems in a rigid body dynamic with cubic integral in velocities. *Results in Physics*, 8:559–568, 2018.

[7] T. S. Amer and W. S. Amer. The substantial condition for the fourth first integral of the rigid body problem. *Mathematics and Mechanics of Solids*, 23(8):1237–1246, 2018.
[8] S. V. Ershkov. A riccati-type solution of euler-poisson equations of rigid body rotation over the fixed point. *Journal of Aerospace Engineering*, 228:2719–2723, 2017.
[9] S. V. Ershkov and D. Leshchenko. On a new type of solving procedure for euler-poisson equations (rigid body rotation over the fixed point). *Acta Mechanica*, 230:871–883, 2019.
[10] S. V. Ershkov and D. D. Leshchenko. On a new type of solving procedure for euler-poisson equations (rigid body rotation over the fixed point). *Acta Mechanica*, 230(1):871–883, 2019.
[11] A. A. Elmandouh. On the stability of the permanent rotations of a charged rigid body-gyrostat. *Acta Mechanica*, 228:3947–3959, 2017.
[12] T. S. Amer, I. M. Abady, H. A. Abdo, and H. F. El-Kafly. The asymptotic solutions for the motion of a charged symmetric gyrostat in the irrational frequency case. *Scientific Reports*, 14:16662, 2024.
[13] T. S. Amer, H. F. El-Kafly, A. H. Elneklawy, and A. A. Galal. Analyzing the spatial motion of a rigid body subjected to constant body-fixed torques and gyrostatic moment. *Scientific Reports*, 14(1):5390, 2024.
[14] T. S. Amer and I. M. Abady. On the motion of a gyro in the presence of a newtonian force field and applied moments. *Mathematics and Mechanics of Solids*, 23(9):1263–1273, 2018.
[15] T. S. Amer. On the rotational motion of a gyrostat with mass distribution. *Nonlinear Dynamics*, 54:189–198, 2008.
[16] T. S. Amer. On the motion of a gyrostat similar to lagrange's gyroscope under the influence of a gyrostatic moment vector. *Nonlinear Dynamics*, 54:249–262, 2008.
[17] M. A. Farag. Analysis of the rotational motion of a solid body in the presence of external moments. *Journal of Vibration Engineering & Technologies*, 12(1):757–771, 2023.
[18] A. I. Ismail. On the application of krylov-bogoliubov-mitropolski technique for treating the motion about a fixed point of a fast spinning heavy solid. *Zeitschrift für Flugwissenschaften und Weltraumforschung (ZFW)*, 20(4):205–208, 1996.
[19] A. I. Ismail. Treating a singular case for a motion of rigid body in a newtonian field of force. *Archive of Mechanics*, 49(6):1091–1101, 1997.
[20] D. D. Leshchenko and A. S. Shamaev. Perturbed rotational motions of a rigid body close to regular precession in the lagrange case. *Izvestiya Akademii Nauk SSSR, Mekhanika Tverdogo Tela*, 22(6):8–17, 1987.
[21] D. D. Leshchenko and S. N. Sallam. Perturbed rotational motions of a rigid body similar to regular precession. *Journal of Applied Mathematics and Mechanics*, 54(2):183–190, 1990.
[22] T. S. Amer. On the rotational motion of a gyrostat with mass distribution. *Nonlinear Dynamics*, 54:189–198, 2008.
[23] T. S. Amer and I. M. Abady. On the motion of a gyro in the presence of a newtonian

force field and applied moments. *Mathematics and Mechanics of Solids*, 23(9):1263–1273, 2018.

[24] A. I. Ismail, T. S. Amer, and S. A. El Banna. Electromagnetic gyroscopic motion. *Journal of Applied Mathematics*, 2012.

[25] T. S. Amer. The rotational motion of the electromagnetic symmetric rigid body. *Applied Mathematics and Information Sciences*, 10(4):1453–1464, 2016.

[26] V. S. Elfimov. Existence of periodic solutions of equations of motion of a solid body similar to the lagrange gyroscope. *Journal of Applied Mathematics and Mechanics*, 42(2):251–258, 1978.

[27] A. I. Ismail. Applying the large parameter technique for solving a slow rotary motion of a disc about a fixed point. *International Journal of Aerospace Engineering*, 2020:7, 2020.

[28] A. I. Ismail. Solving a problem of rotary motion for a heavy solid using the large parameter method. *Advances in Astronomy*, 2020:7, 2020.

[29] E. T. Whittaker. *A Treatise on the Analytical Dynamics of Particles and Rigid Bodies: With an Introduction to the Problem of Three Bodies*. Cambridge University Press, 1988.

[30] P. C. Hughes. *Spacecraft Attitude Dynamics*. Dover Publications, 2004.

[31] J. J. Craig. *Introduction to Robotics: Mechanics and Control*. Springer, 2004.

[32] T. S. Amer, W. S. Amer, M. Fakharany, A. H. Elneklawy, and H. F. El-Kafly. Modeling of the euler-poisson equations for rigid bodies in the context of the gyrostatic influences: An innovative methodology. *European Journal of Pure and Applied Mathematics*, 18(1):5712, 2025.

[33] T. S. Amer, H. A. El-Kafly, A. H. Elneklawy, and W. S. Amer. Modeling analysis on the influence of the gyrostatic moment on the motion of a charged rigid body subjected to constant axial torque. *Journal of Low Frequency Noise, Vibration and Active Control*, 43(4):1593–1610, 2024.

[34] T. S. Amer, A. H. Elneklawy, and H. F. El-Kafly. Analysis of euler's equations for a symmetric rigid body subject to time-dependent gyrostatic torque. *Journal of Low Frequency Noise, Vibration and Active Control*, 2025.

[35] T. S. Amer, H. F. El-Kafly, A. H. Elneklawy, and A. A. Galal. Analyzing the dynamics of a charged rotating rigid body under constant torques. *Scientific Reports*, 14(1):9839, 2024.

[36] A. A. Galal, T. S. Amer, A. H. Elneklawy, and H. F. El-Kafly. Studying the influence of a gyrostatic moment on the motion of a charged rigid body containing a viscous incompressible liquid. *The European Physical Journal Plus*, 138:959, 2023.

[37] F. M. El-Sabaa, T. S. Amer, H. M. Gad, and M. A. Bek. On the motion of a damped rigid body near resonances under the influence of harmonically external force and moments. *Results in Physics*, 19:103352, 2020.

[38] J. Awrejcewicz, R. Starosta, and G. S. Kamińska. Asymptotic analysis of resonances in nonlinear vibrations of the 3-dof pendulum. *Differential Equations and Dynamical Systems*, 21:123–140, 2013.

[39] T. S. Amer, M. A. Bek, and M. K. Abouhmr. On the vibrational analysis for the mo-

tion of a harmonically damped rigid body pendulum. *Nonlinear Dynamics*, 91:2485–2502, 2018.

[40] T. S. Amer. The dynamical behavior of a rigid body relative equilibrium position. *Advances in Mathematical Physics*, 2017:1–13, 2017.

[41] R. W. Hamming. *Numerical Methods for Scientists and Engineers*. Dover Publications, 1987.

[42] I. M. Abady, T. S. Amer, H. M. Gad, and M. A. Bek. The asymptotic analysis and stability of 3dof non-linear damped rigid body pendulum near resonance. *Ain Shams Engineering Journal*, 91(2):101554, 2022.

[43] T. S. Amer, F. M. El-Sabaa, S. K. Zakria, and A. A. Galal. The stability of 3-dof triple-rigid-body pendulum system near resonances. *Nonlinear Dynamics*, 110:1339–1371, 2022.

[44] S. H. Strogatz. *Nonlinear Dynamics and Chaos: With Applications to Physics, Biology, Chemistry, and Engineering*. Princeton University Press, Princeton, 2015.

[45] R. Jarrar, R. Safdar, N. F. Mohammad, O. Florea, and J. Asad. Dynamical node of case study on mass spring system on a massless cart: Compared analytical and numerical solutions. *Journal of Mechanics of Continua and Mathematical Sciences*, 20:1–10, 2025.

[46] O. A. Florea, D. Shahroor, R. Wannan, and J. Asad. Pendulum between two springs using ms-dtm. *Nonlinear Dynamics*, 100(2):025240, 2025.

[47] T. Al-khader, D. K. Maiti, T. Roy, O. Florea, and J. Asad. Time dependent harmonic oscillator via om-hpm. *Journal of Computational and Applied Mechanics*, 56(1):264–275, 2025.

[48] T. Roy, A. Soqi, D. K. Maiti, R. Wannan, and J. Asad. Pendulum attached to a vibrating point: Semi-analytical solution by optimal and modified homotopy perturbation method. *Alexandria Engineering Journal*, 111:396–403, 2025.

[49] T. S. Amer and I. M. Abady. On the application of kbm method for the 3-d motion of asymmetric rigid body. *Nonlinear Dynamics*, 89:1591–1609, 2017.

[50] A. H. Nayfeh. *Introduction to Perturbation Techniques*. Wiley-VCH, 2011.

[51] T. S. Amer, A. H. Elneklawy, and H. F. El-Kafly. Dynamical motion of a spacecraft containing a slug and influenced by a gyrostatic moment and constant torques. *Journal of Low Frequency Noise, Vibration and Active Control*, 2025.

[52] T. S. Amer and I. M. Abady. On the solutions of the euler's dynamic equations for the motion of a rigid body. *Journal of Aerospace Engineering*, 30(4):04017021, 2017.

[53] D. F. Griffiths and D. J. Higham. *Numerical Methods for Ordinary Differential Equations: Initial Value Problems*. Springer, 2010.

[54] T. S. Amer. Motion of a rigid body analogous to the case of euler and poinsot. *Analysis*, 24:305–315, 2004.

[55] T. S. Amer, A. H. Elneklawy, and H. F. El-Kafly. A novel approach to solving euler's nonlinear equations for a 3dof dynamical motion of a rigid body under gyrostatic and constant torques. *Journal of Low Frequency Noise, Vibration and Active Control*, 44(1):111–129, 2025.

Appendix 1

$$\Gamma_{11} = -\tfrac{1}{2}d_2^2[\chi - k\delta(1+\chi\delta)] - \tfrac{1}{br_{10}}\{A_1[b(1+\chi\delta)-1][d_1 - \delta + \delta d_2(k+1)]$$

$$-A_3[b(1+\chi\delta)-1][d_1\chi - 1 - \chi\delta + d_2(k+1)(1+\chi\delta)]$$

$$-A_1A_3[b(1+\chi\delta)-1][\chi + \delta(1+\chi\delta)(k+1)]\} + \tfrac{\acute{\lambda_2}}{\rho_1\rho_2}\{\tfrac{A_2}{b}[b(1+\chi\delta)-1]$$

$$\times[\rho_2(1+\chi\delta) + \chi\delta\rho_1 + \delta^2(1+\chi\delta)(\rho_1+\rho_2)(k+1)] - \tfrac{1}{2\rho_1\rho_2}\delta^2\chi\acute{\lambda_2}r_{10}^2(1$$

$$+\chi\delta)^2(\chi - (k+1)(1+\chi\delta))(\rho_1+\rho_2)^2\},$$

$$\Gamma_{12} = -\tfrac{1}{2}\delta^2[\chi - k\delta(1+\chi\delta)],$$

$$\Gamma_{13} = -\tfrac{1}{2}(1+\chi\delta)^2[\chi - k(1+\chi\delta)],$$

$$\Gamma_{14} = \tfrac{1}{br_{10}}[b(1+\chi\delta)) - 1][d_1 - \delta + \delta d_2(k+1)] - \delta d_2[\chi - k\delta(1+\chi\delta)],$$

$$\Gamma_{15} = \tfrac{1}{br_{10}}[b(1+\chi\delta)) - 1][d_1\chi - 1 - \chi\delta + d_2(1+k)(1+\chi\delta)] - d_2(1+\chi\delta)[\chi - k\delta(1+\chi\delta)],$$

$$\Gamma_{16} = \tfrac{1}{br_{10}}[b(1+\chi\delta)) - 1][\chi + \delta(1+k)(1+\chi\delta)] - \delta(1+\chi\delta)[\chi - k\delta(1+\chi\delta)],$$

$$\Gamma_{17} = \tfrac{\lambda_2}{\rho_1\rho_2}\{\tfrac{[b(1+\chi\delta))-1]}{b}[\rho_2(1+\chi\delta) + \chi\delta\rho_1 + \delta^2(1+\chi\delta)(1+k)(\rho_1+\rho_2)]$$

$$-\delta^2 r_{10}(1+\chi\delta)(\rho_1+\rho_2)(\chi - k\delta(1+\chi\delta))\},$$

$$\Gamma_{18} = \tfrac{\acute{\lambda_2}}{\rho_1\rho_2}\{\tfrac{[b(1+\chi\delta))-1]}{b}\{\chi[\rho_2(1+\chi\delta) + \chi\delta\rho_1] + \delta(1+k)(1+\chi\delta)^2(\rho_1+\rho_2)\}$$

$$-\delta\acute{\lambda_2}r_{10}(1+\chi\delta)^2(\rho_1 + \rho_2)(\chi - \delta k(1+\chi\delta))\},$$

$$\Gamma_{21} = \tfrac{1}{2}d_2^2[k(1+\chi\delta)^2 - \chi^2] - \tfrac{1}{r_{10}}\{A_1[\chi(1+\chi\delta)][d_1 - \delta + \delta d_2(1+k)]$$

$$-A_3[\chi(1+\chi\delta)-1][d_1\chi - 1 - \chi\delta + d_2(1+k)(1+\chi\delta)] - A_1A_3[\chi(1+\chi\delta)][\chi + \delta(1+\chi\delta)(k+1)]\}$$

$$+\tfrac{\chi\acute{\lambda_2}}{\rho_1\rho_2}\{A_2(1+\chi\delta)[\rho_2(1+\chi\delta) + \chi\delta\rho_1 + \delta^2(1+\chi\delta)(1+k)(\rho_1+\rho_2)] - \tfrac{1}{2\rho_1\rho_2}\delta^2\acute{\lambda_2^2}r_{10}^2(1+\chi\delta)^2(\rho_1$$

$$+\rho_2)^2)(k(1+\chi\delta)^2 - \chi^2)\},$$

$$\Gamma_{22} = -\tfrac{1}{2}[k(1+\chi\delta)^2 - \chi^2]\delta^2,$$

$$\Gamma_{23} = -\tfrac{1}{2}(1+\chi\delta)^2[k(1+\chi\delta)^2 - \chi^2],$$

$$\Gamma_{24} = \tfrac{\chi}{r_{10}}\{(1+\chi\delta)[d_1 - \delta + \delta d_2(1+k)] + \delta r_{10}d_2[k(1+\chi\delta)^2 - \chi^2]\},$$

$$\Gamma_{25} = \tfrac{\chi(1+\chi\delta)}{r_{10}}\{[d_1\chi + (1+\chi\delta)(d_2(1+k)-1)] + d_2r_{10}[k(1+\chi\delta)^2 - \chi^2\},$$

$$\Gamma_{26} = \tfrac{\chi}{r_{10}}(1+\chi\delta)\{[\chi + \delta(1+\chi\delta)(1+k)] - \delta r_{10}[(1+\chi\delta)^2 - \chi^2]\},$$

$$\Gamma_{27} = \tfrac{\chi(1+\chi\delta)\acute{\lambda_2}}{\rho_1\rho_2}\{[\rho_2(1+\chi\delta) + \chi\delta\rho_1 + \delta^2(1+\chi\delta)(\rho_1+\rho_2)(1+k)] + \tfrac{\delta^2}{\chi}[k(1+\chi\delta)^2]$$

$$-\chi^2]r_{10}(\rho_1+\rho_2)\},$$

$$\Gamma_{28} = \tfrac{\acute{\lambda_2}\chi(1+\chi\delta)}{\rho_1\rho_2}\{[\chi(\rho_2(1+\chi\delta) + \chi\delta\rho_1) + \delta(1+k)(1+\chi\delta)^2(\rho_1+\rho_2)] + \delta r_{10}(1+\chi\delta)^2$$

$$\times[k(1+\chi\delta)^2 - \chi^2](\rho_1+\rho_2)\},$$

$$\Gamma_{31} = \tfrac{1}{br_{10}}\{A_1(1+\chi\delta)\acute{\lambda_2}[d_1-\delta+\delta d_2(1+k)] + A_3[(1+\chi\delta)\acute{\lambda_2}[d_1\chi$$

$$-1-\chi\delta+d_2(1+\chi\delta)(1+k)]] + A_1A_3[(1+\chi\delta)\acute{\lambda_2}[\chi+\delta(1+\chi\delta)(1+k)]]\} - \tfrac{A_2}{b\rho_1\rho_2}$$

$$\times[(1+\chi\delta)\acute{\lambda_2}^2[\rho_2(1+\chi\delta)+\chi\delta\rho_1+\delta^2(1+k)(1+\chi\delta)(\rho_1+\rho_2)]],$$

$$\Gamma_{32} = 0,$$
$$\Gamma_{33} = 0,$$
$$\Gamma_{34} = -\tfrac{\acute{\lambda_2}}{br_{10}}(1+\chi\delta)[d_1+\delta(d_2(1+k)-1)],$$
$$\Gamma_{35} = -\tfrac{\lambda_2}{br_{10}}\{(1+\chi\delta)[d_1\chi+(1+\chi\delta)(d_2(1+k)-1)]\},$$
$$\Gamma_{36} = -\tfrac{\lambda_2}{br_{10}}(1+\chi\delta)[\chi+\delta(1+k)(1+\chi\delta)],$$
$$\Gamma_{37} = -\tfrac{\lambda_2}{b\rho_1\rho_2}(1+\chi\delta)\{(1+\chi\delta)[\rho_2+\delta^2(\rho_1+\rho_2)(1+k)]+\chi\delta\rho_1\},$$
$$\Gamma_{38} = -\tfrac{\lambda_2}{b\rho_1\rho_2}(1+\chi\delta)\{\chi[\rho_2(1+\chi\delta)+\chi\delta\rho_1]+\delta(1+k)(1+\chi\delta)^2(\rho_1+\rho_2)\},$$
$$\Gamma_{41} = \tfrac{1}{2}d_2^2[\chi d_1+(1+\chi\delta)(1-kd_2)] - \tfrac{1}{br_{10}}\{A_1[ad_1(1+\chi\delta)-\chi d_2]$$
$$\times[d_1-\delta+\delta d_2(k+1)] - A_3[ad_1(1+\chi\delta)-\chi d_2][d_1\chi-1-\chi\delta+d_2(1+k)(1+\chi\delta)]$$
$$-A_1A_3[ad_1(1+\chi\delta)-\chi d_2][\chi+\delta(1+\chi\delta)(1+k)]\} + \tfrac{\acute{\lambda_2}}{\rho_1\rho_2}\{\tfrac{A_2}{b}[ad_1(1$$
$$+\chi\delta)-\chi d_2][\rho_2(1+\chi\delta)+\chi\delta\rho_1+\delta^2(1+\chi\delta)(\rho_1+\rho_2)(1+k)] + \tfrac{1}{2\rho_1\rho_2}\delta^2\acute{\lambda_1^2}r_{10}^2(1+\chi\delta)^2$$
$$\times[\chi d_1+(1+\chi\delta)(1-kd_2)](\rho_1+\rho_2)^2\},$$
$$\Gamma_{42} = \tfrac{1}{2}[\chi d_1+(1+\chi\delta)(1-kd_2)]\delta^2,$$
$$\Gamma_{43} = \tfrac{1}{2}[\chi d_1+(1+\chi\delta)(1-kd_2)](1+\chi\delta)^2,$$
$$\Gamma_{44} = \tfrac{1}{br_{10}}\{[ad_1(1+\chi\delta)-\chi d_2][d_1+\delta(d_2(k+1)-1)]\} + \delta[\chi d_1+(1+\chi\delta)(1-kd_2)]d_2,$$
$$\Gamma_{45} = \tfrac{1}{br_{10}}\{[ad_1(1+\chi\delta)-\chi d_2][d_1\chi+(1+\chi\delta)(d_2(k+1)-1)]\} + (1+\chi\delta)[\chi d_1$$
$$+(1+\chi\delta)(1-kd_2)]d_2,$$
$$\Gamma_{46} = \tfrac{1}{br_{10}}\{[ad_1(1+\chi\delta)-\chi d_2][\chi+\delta(1+\chi\delta)(1+k)]\} + \delta(1+\chi\delta)[\chi d_1+(1+\chi\delta)(1-kd_2)],$$
$$\Gamma_{47} = \tfrac{\lambda_2}{b\rho_1\rho_2}\{[ad_1(1+\chi\delta)-\chi d_2][(1+\chi\delta)(\rho_2+\delta^2(1+k)(\rho_1+\rho_2))+\chi\delta\rho_1]$$
$$+\delta^2(1+k)br_{10}(1+\chi\delta)(\rho_1+\rho_2)+[d_1\chi+(1+\chi\delta)(1-k)d_2]\},$$
$$\Gamma_{48} = \tfrac{\acute{\lambda_2}}{b\rho_1\rho_2}\{[ad_1(1+\chi\delta)-\chi d_2]\{\chi[\rho_2(1+\chi\delta)+\delta\chi\rho_1]+\delta(1+\chi\delta)^2(\rho_1+\rho_2(1+k))$$
$$+\delta br_{10}(1+\chi\delta)^2(\rho_1+\rho_2)[\chi d_1+(1+\chi\delta)(1-kd_2)]\},$$
$$\Gamma_{51} = \tfrac{1}{2}d_2^2(1-\delta^2k) + \tfrac{\delta}{r_{10}}\{A_1[(d_1+\delta((1+k)d_2-1)] + A_3[(d_1\chi-1-\chi\delta)+(1+k)(1+\chi\delta)d_2]$$
$$+A_1A_3[\chi+(1+\chi\delta)\delta(1+k)]\} - \tfrac{\acute{\lambda_2}\delta}{\rho_1\rho_2}\{A_2[\rho_2(1+\chi\delta)+\chi\delta\rho_1+\delta^2(1+\chi\delta)(\rho_1+\rho_2)(k+1)]$$
$$+\tfrac{1}{2\rho_1\rho_2}\delta r_{10}^2\acute{\lambda_2^2}(1+\chi\delta)^2(\rho_1+\rho_2)^2(1-k\delta^2)\},$$
$$\Gamma_{52} = \tfrac{1}{2}\delta^2(1-k\delta^2),$$

$$\Gamma_{53} = \tfrac{1}{2}(1+\chi\delta)^2(1-k\delta^2),$$
$$\Gamma_{54} = \tfrac{\delta}{r_{10}}[d_2(r_{10}(1-k\delta^2) - \delta(k+1)) + \delta - d_1],$$
$$\Gamma_{55} = d_2(1+\chi\delta)(1-k\delta^2) - \tfrac{\delta}{r_{10}}[(1+\chi\delta)(d_2(1+k)+1) - d_1\chi],$$
$$\Gamma_{56} = \tfrac{\delta}{r_{10}}[(1+\chi\delta)(1-\delta(1+k)) - \chi] + \delta(1+\chi\delta)(1-k\delta^2),$$
$$\Gamma_{57} = \tfrac{\lambda_2\delta}{\rho_1\rho_2}\{[\rho_2(1+\chi\delta) + \chi\rho_1 + \delta(\rho_1+\rho_2)(1+\chi\delta)(k+1)]] + \delta r_{10}(1+\chi\delta)(\rho_1+\rho_2)(1-k\delta^2)\},$$
$$\Gamma_{58} = \tfrac{\lambda_2\delta}{\rho_1\rho_2}(\rho_1+\rho_2)\{\delta r_{10}(1-k\delta^2)(1+\chi\delta)^2 - [(1+\chi\delta)^2(1+k) + \chi\delta[\rho_2(1+\chi\delta) + \chi\delta\rho_1]]\},$$
$$\Gamma_{61} = \tfrac{1}{br_{10}}\{[d_1 + \delta(d_2(k+1)-1)](1+b\chi\delta)A_1 + (1+b\chi\delta)[(1+\chi\delta)(d_2(k+1)-1) + d_1\chi]A_3$$
$$+(1+b\chi\delta)[\chi + \delta(k+1)(1+\chi\delta)]A_1A_3\}$$
$$+\tfrac{d_2^2}{2}(\chi - k\delta(1+\delta\chi)) - \tfrac{\acute{\lambda_2}}{b\rho_1\rho_2}(1+b\chi\delta)[\rho_2(1+\chi\delta) + \chi\delta\rho_1 + (\rho_1+\rho_2)$$
$$\times\delta^2(1+\chi\delta)(k+1)]A_3 + \tfrac{\delta^2}{2}(\chi - k\delta(1+\chi\delta))(\tfrac{\acute{\lambda_2}A_2r_{10}}{\rho_1\rho_2})^2(1+\chi\delta)^2(\rho_1+\rho_2)^2],$$
$$\Gamma_{62} = \tfrac{\delta^2}{2}(\chi - k\delta(1+\chi\delta)),$$
$$\Gamma_{63} = \tfrac{(1+\chi\delta)^2}{2}(\chi - k\delta(1+\chi\delta)),$$
$$\Gamma_{64} = -\tfrac{1}{br_{10}}[d_1 - \delta(1-d_2(1+k))](1+b\chi\delta) + \delta(\chi - k\delta(1+\chi\delta))d_2,$$
$$\Gamma_{65} = -\tfrac{1}{br_{10}}(1+b\chi\delta)[(1+\chi\delta)(d_2(k+1)-1) + \chi d_1] + (1+\chi\delta)(\chi - k\delta(1+\chi\delta)))d_2,$$
$$\Gamma_{66} = -\tfrac{1}{br_{10}}[\chi + \delta(k+1)(1+\chi\delta)](1+b\chi\delta) + \delta(1+\chi\delta)(\chi - k\delta(1+\chi\delta)),$$
$$\Gamma_{67} = -\tfrac{\lambda_2}{b\rho_1\rho_2}\{(1+b\chi\delta)[\rho_2(1+\chi\delta) + \chi\delta\rho_1 + \delta^2(1+\chi\delta)(\rho_1+\rho_2)(k+1)]$$
$$-\delta^2br_{10}(1+\chi\delta)(\chi - k\delta(1+\chi\delta))(\rho_1+\rho_2)\},$$
$$\Gamma_{68} = -\tfrac{\acute{\lambda_2}}{b\rho_1\rho_2}\{\chi(1+b\chi\delta)[(\rho_1+\rho_2)\chi\delta + \rho_2] + \delta(1+\chi\delta)^2(k+1)(\rho_1+\rho_2)]$$
$$+\delta br_{10}(1+\chi\delta)^2(\chi - k\delta(1+\chi\delta))(\rho_1+\rho_2)\},$$
$$\Gamma_{71} = -\tfrac{\delta\acute{\lambda_2}[d_1-\delta+\delta d_2(k+1)]}{br_{10}}A_1 - \tfrac{\delta\acute{\lambda_2}[d_1\chi-(1+\chi\delta)(d_2(1+k)-1)]}{br_{10}}A_3$$
$$-\tfrac{\delta\acute{\lambda_2}[\chi+\delta(1+k)(1+\chi\delta)]}{br_{10}}A_1A_3 + \tfrac{\delta\acute{\lambda_2}^2}{b\rho_1\rho_2}[\delta\chi\rho_1 + (1+\chi\delta)\rho_2 + \delta^2$$
$$\times(1+\chi\delta)(\rho_1+\rho_2)(k+1)]A_2,$$
$$\Gamma_{72} = 0,$$
$$\Gamma_{73} = 0,$$
$$\Gamma_{74} = \tfrac{\delta\acute{\lambda_2}[(d_1-\delta)+\delta d_2(k+1)]}{br_{10}},$$
$$\Gamma_{75} = \tfrac{\delta\acute{\lambda_2}[d_2(1+\chi\delta)(k+1)+(d_1\chi-(1+\chi\delta))]}{br_{10}},$$
$$\Gamma_{76} = \tfrac{\delta\acute{\lambda_2}}{br_{10}}[\chi + \delta(1+\chi\delta)(k+1)],$$
$$\Gamma_{77} = \tfrac{\delta\acute{\lambda_2}^2}{b\rho_1\rho_2}[\chi\delta\rho_1 + \rho_2(1+\chi\delta) + \delta^2(1+\chi\delta)(k+1)(\rho_1+\rho_2)],$$
$$\Gamma_{78} = \tfrac{\delta\acute{\lambda_2}^2}{b\rho_1\rho_2}\{\chi[\chi\delta\rho_1 + \rho_2(1+\chi\delta)] + \delta(1+\chi\delta)^2(\rho_1+\rho_2)(k+1)\},$$

$$\Gamma_{81} = -\frac{[(d_1-\delta)+\delta d_2(k+1)][d_2-\delta a d_1)]}{br_{10}}A_1 - \frac{1}{br_{10}}[(d_1\chi-(1+\chi\delta))$$

$$+d_2(1+\chi\delta)(k+1)][d_2-\delta a d_1]A_3 - \frac{1}{2}(d_1+\delta(1-kd_2))d_2^2$$

$$+\frac{[\chi+\delta(1+\chi\delta)(k+1)][d_2-\delta a d_1]}{br_{10}}A_1A_3 + \frac{\acute{\lambda_2}}{b\rho_1\rho_2}[\chi\delta\rho_1+\rho_2(1+\chi\delta)+\delta^2$$

$$\times(1+\chi\delta)(\rho_1+\rho_2)(k+1)][d_2-\delta a d_1]A_2 - \frac{1}{2}\frac{\delta^2\acute{\lambda_2}^2 r_{10}^2(1+\chi\delta)^2}{(\rho_1\rho_2)^2}(d_1$$

$$+\delta(1-kd_2))(\rho_1+\rho_2)^2,$$

$$\Gamma_{82} = -\frac{\delta^2}{2}(d_1+\delta(1-kd_2)),$$

$$\Gamma_{83} = -\frac{(1+\chi\delta)^2}{2}(d_1+\delta(1-kd_2)),$$

$$\Gamma_{84} = \frac{[(d_1-\delta)+\delta d_2][d_2-\delta(ad_1+\acute{\lambda_1})]}{br_{10}} - \delta d_2(d_1+\delta),$$

$$\Gamma_{85} = \frac{1}{br_{10}}[(d_1\chi-(1+\chi\delta))+(1+\chi\delta)d_2(k+1)][d_2-\delta a d_1] - d_2(1+\chi\delta)$$
$$\times(d_1+\delta(1-kd_2)),$$

$$\Gamma_{86} = \frac{[\chi+\delta(k+1)(1+\chi\delta)][d_2-\delta a d_1]}{br_{10}} - \delta(1+\chi\delta)(d_1+\delta(1-kd_2)),$$

$$\Gamma_{87} = \frac{\acute{\lambda_2}}{b\rho_1\rho_2}[(1+\chi\delta)\rho_2+\chi\delta\rho_1+\delta^2(k+1)(1+\chi\delta)(\rho_1+\rho_2)][d_2-\delta a d_1]$$
$$-\frac{\delta^2\lambda_2 r_{10}}{\rho_1\rho_2}(1+\chi\delta)(\rho_1+\rho_2)(d_1+\delta(1-kd_2)),$$

$$\Gamma_{88} = \frac{\lambda_2}{b\rho_1\rho_2}\{\chi[\rho_1\chi\delta+(1+\chi\delta)\rho_2]+\delta(1+\chi\delta)^2(\rho_1+\rho_2)(k+1)\}[d_2-\delta a d_1]$$

$$-\frac{\delta\acute{\lambda_2}r_{10}(1+\chi\delta)^2}{\rho_1\rho_2}(\rho_1+\rho_2)(d_1+\delta(1-kd_2)),$$

Appendix2

$$
\begin{aligned}
G_{10} &= \Gamma_{41} + \tfrac{1}{2}[(2\Gamma_{42} - \Gamma_{41})(A_1^2 + A_2^2) + (2\Gamma_{43} - \Gamma_{25})A_3^2] - 2\Gamma_{17}A_1A_2,\\
G_{11} &= \Gamma_{44} - 2\Gamma_{11} - 2(A_1^2 + A_2^2)\Gamma_{12} - \tfrac{1}{2}[4\Gamma_{13} + \tfrac{1}{\rho_1}(\rho_1 + \rho_2)\Gamma_{26}]A_3^2 - 2\\
&\quad \times\rho_1\mu_0 - \tfrac{\acute{\lambda_2}r_{10}(1+\chi\delta)}{\rho_1}\Gamma_{17} - \tfrac{\acute{\lambda_2}r_{10}\delta}{\rho_2}\Gamma_{27} + \Gamma_{37},\\
G_{12} &= \tfrac{1}{2\rho_1}(\rho_1 - \rho_2)A_3^2\Gamma_{26},\\
G_{13} &= -\tfrac{3}{2}(A_1^2 - A_2^2)\Gamma_{14} + A_1A_2\Gamma_{17},\\
G_{14} &= -3A_1A_2\Gamma_{14} - \tfrac{1}{2}\Gamma_{17}(3A_1^2 - A_2^2) - \tfrac{1}{2\rho_1}(\rho_1 + \rho_2)A_1A_2\Gamma_{27},\\
G_{15} &= \Gamma_{45} - \tfrac{1}{2}(3 - \tfrac{\rho_2}{\rho_1})(A_1^2 - A_2^2)\Gamma_{16} - \tfrac{1}{\rho_1}(\rho_1 + \rho_2)[\Gamma_{21} + A_3^2\Gamma_{23}\\
&\quad +(A_1^2 + A_2^2)\Gamma_{22}] - \tfrac{\acute{\lambda_2}r_{10}\delta}{\rho_1}\Gamma_{28} + \tfrac{\rho_2}{\rho_1}[\Gamma_{38} - \tfrac{\acute{\lambda_2}r_{10}(1+\chi\delta)}{\rho_1}\Gamma_{18}],\\
G_{16} &= \Gamma_{46} - \tfrac{1}{2}[2\Gamma_{15} + \tfrac{1}{\rho_1}(\rho_1 + \rho_2)\Gamma_{24}],\\
G_{17} &= -\tfrac{1}{2}(\Gamma_{24} + \tfrac{\rho_2}{\rho_1}\Gamma_{15}),\\
G_{18} &= -\tfrac{1}{2}[2\Gamma_{15} + \tfrac{1}{\rho_1}(\rho_1 + \rho_2)\Gamma_{24}),\\
G_{19} &= \tfrac{\rho_2}{2\rho_1}\Gamma_{15} + \tfrac{1}{2}\Gamma_{24},\\
G_{110} &= \tfrac{1}{2}\Gamma_{61}A_3[\tfrac{1}{\rho_1}(\rho_1 - \rho_2)A_1^2 - 2(A_1^2 + A_2^2)],\\
G_{111} &= -(3 - \tfrac{\rho_2}{\rho_1})A_1A_2A_3\Gamma_{16},\\
G_{112} &= -\tfrac{1}{2\rho_1}(\rho_1 + \rho_2)\Gamma_{26},\\
G_{113} &= -\tfrac{1}{2\rho_1}(\rho_1 - \rho_2)\Gamma_{26},\\
G_{114} &= -\tfrac{1}{2\rho_1}(\rho_1 + \rho_2)A_3^2\Gamma_{25},\\
G_{115} &= -\tfrac{1}{2\rho_1}(\rho_1 + 2\rho_2)A_3^2\Gamma_{28},\\
G_{116} &= -\tfrac{1}{\rho_1}(\rho_1 - \rho_2)\Gamma_{36} - (1 + \tfrac{\rho_2}{2\rho_1})\Gamma_{18} + \tfrac{1}{2\rho_1}(\rho_1 - \rho_2)\tfrac{\acute{\lambda_2}r_{10}\delta}{\rho_2}\Gamma_{26},\\
G_{117} &= -\tfrac{1}{2}[\tfrac{1}{\rho_1}(\rho_1 - \rho_2) - 1]\Gamma_{27},\\
G_{118} &= -\tfrac{1}{2}\Gamma_{27} - \tfrac{1}{2\rho_1}(\rho_1 + \rho_2)\Gamma_{27} - \Gamma_{18},\\
G_{119} &= -\tfrac{\rho_2}{2\rho_1}\Gamma_{18},\\
G_{120} &= -\tfrac{1}{2\rho_1}(\rho_1 + \rho_2)\Gamma_{27},\\
G_{121} &= \Gamma_{47} + \tfrac{\acute{\lambda_2}r_{10}\delta}{\rho_2}\Gamma_{24} + \tfrac{\acute{\lambda_2}r_{10}(1+\chi\delta)}{\rho_1}\Gamma_{14} - \Gamma_{34},\\
G_{122} &= \Gamma_{48} + \tfrac{\acute{\lambda_2}r_{10}\delta}{\rho_1}\Gamma_{25} + \tfrac{\rho_2}{\rho_1}\tfrac{\acute{\lambda_2}r_{10}(1+\chi\delta)}{\rho_1}\Gamma_{15} - \tfrac{\rho_2}{\rho_1}\Gamma_{35},\\
G_{123} &= (1 - \tfrac{\rho_2}{\rho_1})\tfrac{\acute{\lambda_2}r_{10}(1+\chi\delta)}{\rho_1}A_1A_3\Gamma_{16},
\end{aligned}
$$

$$
\begin{aligned}
G_{20} &= -2r_{10}\acute{\lambda_2}\mu_0(1+\chi\delta) + [\Gamma_{11} + (A_1^2+A_2^2)\Gamma_{12} + A_3^2\Gamma_{13}]\tfrac{\acute{\lambda_2}r_{10}(1+\chi\delta)}{\rho_1} + \tfrac{1}{2}A_3^2\Gamma_{28} + [\Gamma_{21}\\
&\quad +(A_1^2+A_2^2)\Gamma_{22} + A_3^2\Gamma_{23}]\tfrac{\acute{\lambda_2}r_{10}\delta}{\rho_2} - [\Gamma_{31} + (A_1^2+A_2^2)\Gamma_{32} + A_3^2\Gamma_{33}] - (A_1^2+A_2^2)\Gamma_{17},\\
G_{21} &= -2\rho_1\mu_0 - 2[\Gamma_{11} + (A_1^2+A_2^2)\Gamma_{12} + A_3^2\Gamma_{13}] - \tfrac{\acute{\lambda_2}r_{10}\delta}{\rho_2}\Gamma_{27} - \tfrac{1}{2}(1-\tfrac{\rho_2}{\rho_1})A_3^2\Gamma_{26}\\
&\quad +\Gamma_{37} + \Gamma_{44} - \tfrac{2\acute{\lambda_2}r_{10}(1+\chi\delta)}{\rho_1}\Gamma_{17},\\
G_{22} &= -\Gamma_{34} + \Gamma_{47} + \tfrac{\acute{\lambda_2}r_{10}\delta}{\rho_2}\Gamma_{24} - \tfrac{2(1+\chi\delta)\acute{\lambda_2}r_{10}}{\rho_1}\Gamma_{14},\\
G_{23} &= \tfrac{1}{2\rho_1}(\rho_1+\rho_2)A_3^2\Gamma_{26},\\
G_{24} &= \tfrac{\rho_2}{2\rho_1}(A_1^2+A_2^2)\Gamma_{16} + \tfrac{\rho_2}{\rho_1}\Gamma_{45} - \tfrac{\acute{\lambda_2}r_{10}\delta}{\rho_2}\Gamma_{28} + \tfrac{2(1+\chi\delta)\acute{\lambda_2}r_{10}}{\rho_1}\Gamma_{18} + \Gamma_{38}\\
&\quad -(1+\tfrac{\rho_2}{\rho_1})[\Gamma_{21} + (A_1^2+A_2^2)\Gamma_{22} + A_3^2\Gamma_{23}],\\
G_{25} &= \tfrac{1}{2}(\Gamma_{15}-\Gamma_{24}) + \tfrac{1}{\rho_1}(\rho_1-\rho_2)\Gamma_{46},\\
G_{26} &= \tfrac{1}{2}[\Gamma_{18} - (1+\tfrac{\rho_2}{\rho_1})\Gamma_{27}],\\
G_{27} &= -\tfrac{1}{2}(\Gamma_{27} + \tfrac{\rho_2}{\rho_1}\Gamma_{18}) + \tfrac{\acute{\lambda_2}r_{10}\delta}{\rho_2}\Gamma_{26} - \tfrac{2(1+\chi\delta)\acute{\lambda_2}r_{10}}{\rho_1}\Gamma_{16} - \Gamma_{36},\\
G_{28} &= -\tfrac{1}{2}(1+\tfrac{\rho_2}{\rho_1})\Gamma_{24} - \tfrac{\rho_2}{2\rho_1}\Gamma_{15},\\
G_{29} &= \tfrac{1}{2}(\Gamma_{15}-\Gamma_{24}),\\
G_{210} &= \tfrac{1}{2\rho_1}[(\rho_1+\rho_2)\Gamma_{24} + \rho_2\Gamma_{15}],\\
G_{211} &= \tfrac{1}{2}[-\Gamma_{18} + (1+\tfrac{\rho_2}{\rho_1})\Gamma_{27}],\\
G_{212} &= -\tfrac{1}{2}[\tfrac{\rho_2}{\rho_1}\Gamma_{18} + \Gamma_{27}],\\
G_{213} &= \tfrac{1}{2\rho_1}(2\rho_1-\rho_2)(A_2^2-A_1^2)A_3\Gamma_{16},\\
G_{214} &= -\tfrac{1}{2\rho_1}(\rho_1+\rho_2)\Gamma_{26},\\
G_{215} &= \tfrac{1}{2\rho_1}(\rho_1-\rho_2)\Gamma_{26},\\
G_{216} &= \tfrac{1}{2}A_3^2\Gamma_{25},\\
G_{217} &= \tfrac{1}{\rho_1}(\rho_1-\rho_2)A_1A_2\Gamma_{16} - \tfrac{\rho_2}{\rho_1}\Gamma_{18} + \tfrac{\delta\acute{\lambda_2}r_{10}}{\rho_2}\Gamma_{25} - \tfrac{2(1+\chi\delta)\acute{\lambda_2}r_{10}}{\rho_1}\Gamma_{15} - \Gamma_{35},\\
G_{218} &= -\tfrac{1}{2}(1+\tfrac{2\rho_2}{\rho_1})\Gamma_{28},\\
G_{32} &= \Gamma_{85} - 2(\rho_2\mu_0 + \Gamma_{61} + \Gamma_{63}A_3^2) - \tfrac{\delta\acute{\lambda_2}r_{10}}{\rho_2}\Gamma_{68} - \tfrac{(1+\chi\delta)\acute{\lambda_2}r_{10}}{\rho_1}\Gamma_{58} + \Gamma_{78},\\
G_{33} &= -\tfrac{3}{2}\Gamma_{68},\\
G_{34} &= -\tfrac{1}{2}\Gamma_{65},\\
G_{40} &= 2\delta\acute{\lambda_2}r_{10}\mu_0 + \tfrac{\delta\acute{\lambda_2}r_{10}}{\rho_2}[\Gamma_{61} + (A_1^2+A_2^2)\Gamma_{62} + A_3^2\Gamma_{63}] + (1+\tfrac{\rho_1}{\rho_2})\tfrac{(1+\chi\delta)\acute{\lambda_2}r_{10}}{\rho_1}\\
&\quad -\tfrac{(1+\chi\delta)\acute{\lambda_2}r_{10}}{\rho_2}[\Gamma_{51} + (A_1^2+A_2^2)\Gamma_{52} + A_3^2\Gamma_{53}] - [\Gamma_{71} + (A_1^2+A_2^2)\Gamma_{72} + A_3^2\Gamma_{73}]\\
&\quad +\tfrac{1}{2}A_3^2\Gamma_{68}] - \tfrac{\rho_1}{2\rho_2}(A_1^2+A_2^2)\Gamma_{57},\\
G_{41} &= -\tfrac{\delta\acute{\lambda_2}r_{10}}{\rho_2}\Gamma_{67} - (1+\tfrac{\rho_1}{\rho_2}) + \tfrac{(1+\chi\delta)\acute{\lambda_2}r_{10}}{\rho_2}\Gamma_{57} + \tfrac{1}{2}(1-\tfrac{\rho_1}{\rho_2})A_3^2\Gamma_{66}\\
&\quad +\Gamma_{77} + \tfrac{\rho_1}{\rho_2}\Gamma_{84},\\
G_{42} &= A_3^2\Gamma_{66},\\
G_{43} &= \tfrac{\delta\acute{\lambda_2}r_{10}}{\rho_2}\Gamma_{64} - \tfrac{(1+\chi\delta)\acute{\lambda_2}r_{10}}{\rho_2}\Gamma_{54} + \tfrac{\rho_1}{\rho_2}\Gamma_{87} - \Gamma_{74},\\
G_{44} &= -\tfrac{\rho_1}{2\rho_2}(A_1^2-A_2^2)\Gamma_{54} + \tfrac{\rho_1}{\rho_2}A_1A_2\Gamma_{57},\\
G_{45} &= -\tfrac{\rho_1}{2\rho_2}(A_1^2-A_2^2)\Gamma_{57} - \tfrac{\rho_1}{\rho_2}A_1A_2\Gamma_{54},\\
G_{46} &= -4\rho_2\mu_0 - 2[\Gamma_{61} + (A_1^2+A_2^2)\Gamma_{62} + A_3^2\Gamma_{63}] + \tfrac{\delta\acute{\lambda_2}r_{10}}{\rho_2}(\Gamma_{56}\\
&\quad -2\Gamma_{68}) + \Gamma_{85} + \Gamma_{78} - \tfrac{1}{2}(1-\tfrac{\rho_1}{\rho_2})(A_1^2+A_2^2)\Gamma_{56} + \tfrac{(1+\chi\delta)\acute{\lambda_2}r_{10}}{\rho_1}\Gamma_{58},\\
G_{47} &= -\tfrac{\rho_1}{2\rho_2}\Gamma_{64} - (1-\tfrac{\rho_1}{\rho_2})\Gamma_{86},\\
G_{48} &= -\tfrac{1}{2}(2\Gamma_{64} + \Gamma_{55}),\\
G_{49} &= \tfrac{\delta\acute{\lambda_2}r_{10}}{\rho_2}\Gamma_{66} - (\Gamma_{76} + \tfrac{1}{2}\Gamma_{58}) - \tfrac{(1+\chi\delta)\acute{\lambda_2}r_{10}}{\rho_2}\Gamma_{56} - \tfrac{\rho_1}{2\rho_2}\Gamma_{67},
\end{aligned}
$$

$$
\begin{aligned}
G_{410} &= -\Gamma_{67},\\
G_{411} &= -\tfrac{\rho_1}{2\rho_2}\Gamma_{64},\\
G_{412} &= \tfrac{1}{2}(2\Gamma_{64}+\Gamma_{55}),\\
G_{413} &= -\tfrac{1}{2}(\Gamma_{58}+\tfrac{\rho_1}{\rho_2}\Gamma_{67}),\\
G_{414} &= -\Gamma_{67},\\
G_{415} &= -\tfrac{1}{2\rho_2}(\rho_2-\rho_1)(A_1^2-A_2^2)A_3\Gamma_{56},\\
G_{416} &= 0,\\
G_{417} &= \tfrac{1}{2\rho_2}(\rho_2-\rho_1)\Gamma_{66},\\
G_{418} &= -\Gamma_{66},\\
G_{419} &= -\tfrac{3}{2}A_3^2\Gamma_{65},\\
G_{420} &= \tfrac{\delta\acute{\lambda_2}r_{10}}{\rho_2}\Gamma_{65}+\Gamma_{88}-\Gamma_{75}-\tfrac{(1+\chi\delta)\acute{\lambda_2}r_{10}}{\rho_1}\Gamma_{55}+(1-\tfrac{\rho_1}{\rho_2})A_1A_2\Gamma_{56},\\
G_{421} &= -\tfrac{3}{2}A_3^2\Gamma_{68},
\end{aligned}
$$